國 立 交 通 大 學

機械工程學系

碩士論文

3D 聲音訊號處理實現於汽車音訊:以單麥克風背景噪音估測為基礎之適應性音訊增益控制器

3D Audio Signal Processing on Automotive Audio: Adaptive Audio Gain Controller Based on One-Microphone Noise Level Estimation

研 究 生: 艾學安

指導教授: 白明憲

中華民國九十八年七月

3D 聲音訊號處理實現於汽車音訊:以單麥克風背景噪音估測為基礎之適應性音訊增益控制器

3D Audio Signal Processing on Automotive Audio: Adaptive Audio Gain Controller Based on One-Microphone Noise Level Estimation

研 究 生：艾學安　　Student：Shie-An Ai

指導教授：白明憲　　Advisor：Mingsian R. Bai

A thesis
Submitted to Department of Mechanical Engineering
Collage of Engineering
National Chiao Tung University
In Partial Fulfillment of Requirements
for the Degree of Master of Science
in
Mechanical Engineering
July 2009
HsinChu, Taiwan, Republic of China

中華民國九十八年七月

3D 聲音訊號處理實現於汽車音訊:以單麥克風背景噪音估測為基礎之適應性音訊增益控制器

研究生：艾學安　　指導教授：白明憲 教授

國立交通大學 機械工程學系 碩士班

摘　　要

本論文的研究著重於提升汽車音訊的聆聽品質。現今車內的多聲道視聽系統進展的十分快速，然而，汽車內部仍然因為一些背景噪音像引擎、震動、冷氣而被視為不良的聆聽環境。再來敘述一些可以在車內惡劣環境下拓展頻寬以及提升聆聽品質的聲音系統。本研究提出三個方法在車內產生聲音特效，第一、二部份分別敘述虛擬重低音(VB)以及語音清晰化(VC)的方法，它們分別闡述將頻寬往低頻拓展以及強調中頻的技術。第三部份提出聲道拓展/壓縮，提出如何針對狹小且反射多的環境提供較好的聲場。本研究也提出了一個新的系統，運用噪音估測系統(NLE)結合動態控制系統(DRC)來適應性的調整汽車音訊系統的增益。此方法運用了兩個系統，首先使用最小均方(LMS)演算法來估測背景噪音的大小，之後計算先驗的訊噪比(SNR)再根據事先設計的靜態曲線(Static curve)可以得到適應性調整後的增益。

3D Audio Signal Processing on Automotive Audio: Adaptive Audio Gain Controller Based on One-Microphone Noise Level Estimation

Student: Shie-An Ai **Advisor: Mingsian R. Bai**

Department of Mechanical Engineering
National Chiao-Tung University

ABSTRACT

A comprehensive study was conducted to improve the listening quality of automotive audio. There is increased proliferation nowadays of multichannel audiovisual systems used in cars. However, the interior of a car is known as a notorious listening environment due to background noise like engine, vibration and air conditioning. It is then desirable to develop audio systems that are capable of extending the bandwidth and improving the audio quality in harsh car environments. This study brings three approaches to generate the audio effect in a car. First and second section is virtual bass (VB) and voice clarity (VC), describes the bandwidth expansion toward the low-frequency and emphasizes the middle-frequency. Third section is updownmix, describes how to render spatial sound field to cope with the reflections in the confined space. This study also proposes a new system that makes use of a Noise Level Estimator (NLE) combines Dynamic Range Control (DRC) to adaptively adjust the gain of an automotive audio system. NLE and DRC are used in the system for noise estimation and automatic gain control, respectively. The system needs one microphone to receive the noisy signal. Background noise level is estimated by a system that uses Least-Mean-Squares (LMS) algorithm and then

calculated *a priori* signal to noise ratio (SNR). According to the static curve designed in advance, the gain of the audio input can be adjusted dynamically based on the SNR determined. These processing algorithms have been practically implemented on a car. Simulations and experiments were conducted for validating the proposed adaptive audio gain control systems.

誌謝

短短兩年的研究生生涯轉眼即逝。在此感謝白明憲教授的諄諄教誨與照顧，在白明憲教授的指導期間，深刻的感受到教授對於追求學問的熱忱，更是佩服教授淵博的學問與解決問題的方法。在教授豐富的專業知識以及嚴謹的治學態度下，使我能夠順利完成學業與論文，在此致上最誠摯的謝意。

在論文寫作方面，感謝本系陳宗麟教授和鄭泗東教授在百忙中撥冗閱讀，並提出寶貴的意見與指導，使得本文的內容更趨完善與充實，在此學生致上無限的感激。

在這兩年的研究生生涯中，承蒙博士班陳榮亮學長、林家鴻學長，以及已畢業的李志中學長、施毗宇學長、洪志仁學長、謝秉儒學長、劉青育學長、黃兆民學長在研究與學業上的適時指點，並有幸與王俊仁同學、郭育志同學、何克男同學、劉冠良同學互相切磋討論，讓我獲益甚多。此外學弟妹陳俊宏、廖國志、廖士涵、曾智文、桂振益、張濬閣、劉嬰婷以及學姐李雨容在生活上的朝夕相處與砥礪磨練，亦值得細細回憶。並且感謝昔日同學偉豪、子睿、建凱、東垣、博群在我困惑的時候同我一起奮鬥，因為有了你們，讓實驗室裡總是充滿歡笑。能順利取得碩士學位，要感謝的人很多，上述名單恐有疏漏，在此一併致上我最深的謝意。

最後僅以此篇論文，獻給我摯愛的家人，奶奶楊光珍女士、母親陳秀華女士、父親艾武先生，這一路上，因為有你們的付出與支持，給了我最大的精神支柱，也讓我有勇氣面對更艱難的挑戰。

TABLE OF CONTENTS

LIST OF TABLES

LIST OF FIGURES

1 INTRODUCTION

With rapid growth in digital telecommunication and display technologies, multimedia audiovisual presentation has become reality for automobiles. However, there remain numerous challenges in automotive audio reproduction due to the notorious nature of the automotive listening environment. This study proposed bandwidth extension (BEW) algorithms and up/downmix algorithms to create a more ambience listening feel. And also, proposed an adaptive audio gain controller (AGC) to enhance the listening environment.

This study presents an approach of adaptive gain controller. Two systems are described in this study. System identification with LMS algorithm is employed to determine the unknown plant. NLE system is used to estimate the background noise. The DRC system is employed to obtain the output gain mapping.

With the increased proliferation nowadays of automotive audio systems, the interior of a car is also known as a notorious listening environment due to engine, vibration, wind and air conditioning. The background noise causes an unclear music. This motivates the current research to develop an adaptive gain controller (AGC) to maintain a stable signal to noise ratio (SNR) for vehicles. The AGC is also used in speech processing [1] and hearing aids. Speech processing in an ambient noise environment uses Artificial Neural Network (ANN) to train the weighting in different noise conditions [2]. Another method used optimal nonlinear filtering of the short-time spectral amplitude (STSA) envelope [3]. For the hearing aids, it is achieved by using two control voltages to determine the gain. One changes slowly as the input varies in level. The other comes into operation when an intense transient occurs [4]. However, those approaches are not considered as a suitable technique for automotive audio. The key issue is the complex processing, which limits its implementation in practical systems. NLE achieved by LMS algorithm is

considering as an efficiency method for noise estimation. NLE combines DRC approach will be presented in this study.

In order to achieve the noise estimation processing, the plant in a car environment need to be determined. The adaptive filter [5], [6] is quite important because its capability to track an unknown system. LMS [7]-[9] and Recursive-Least-Squares (RLS) are two popular algorithms for adaptive filtering. In comparison, LMS has better tracking ability, while RLS has faster convergence speed. The LMS technique possesses the advantages of simplicity in its underlying structure, computational efficiency, and robustness. Therefore, the LMS approach will be presented in this study. However, we still need a DRC system [10]-[13] to accomplish the process. DRC is described by their static and dynamic characteristics. Static characteristics describe the DRC output response to constant level signal. The static characteristics are typically split into four sections: expansion, no-action, compression and limiting. The regions are separated by threshold signal levels. Each characteristic is affected by its slope.

The proposed approaches have been implemented on a real car using a fixed-point digital signal processor (DSP), one microphone and the loudspeakers installed in the cars. The simulation results and the experiment setup will be discussed in this study.

2 BANDWIDTH EXTENSION

Bandwidth extension (BWE) refers to methods that increase the frequency bandwidth of signals. It is desired when the frequency content of the signal at some point should be enhanced to improve audio effects or if the bandwidth of signal has been reduced because of some economical constraints. An obvious way to categorize various BWE methods is based on the frequency range of interest (high

frequency or low frequency) and where the signal bandwidth is actually extended (physical or psycho-acoustical extension) [14]. The psycho-acoustical extension, different to physical BWE, use no practical implementation to contain the frequency range of interest, but exploit the property of human hearing to achieve bandwidth extension. In this study, we described three kinds of BWE applications respectively virtual bass (VB) and voice clarity (VC).

The first application refers to the virtual bass technology, it focuses on how to increase bass enhancement using a loudspeaker which has no low-frequency capability such as a cell phone. A common solution to this problem is to use equalizers that make use of shelving filters or other electronic means, but it does not usually get a good result. If the power amplifier and the loudspeaker are not redesigned for the low-frequency purpose, boosting bass directly will cause distortions or even permanent damage. To overcome the above-mentioned problems, the virtual bass technology exploits a psycho-acoustic property of human hearing that humans are capable of “extrapolating” the missing fundamental in the low frequency range based on higher harmonics. The pitch-shifting algorithm of phase vocoder can realize the concept by modifying the phase properly, and then the equal loudness contour is exploited to adjust the loudness [15]. Instead of generating harmonics by pitch-shifting algorithm which requires a complex calculation of phase [16], nonlinear processing can create new bandwidth more efficiently and conveniently. Even if the fundamental frequency is missing, it will still perceived as a residue pitch, which in this case is sometimes called ‘virtual pitch’ or ‘missing fundamental.’ Finally, we use the implementation of multistage up/down-sampling structure to save evaluation [17]. The second application refers to the voice clarity technology; it is requested when the speech is not clarified enough for listening. This problem is probably because of the low loudness of voice we want to listen or the loud

background music. It usually happens as someone watching movies or talking by telephone. In this study we aim to overcome the problem by some simple algorithms including nonlinear processing.

Because it is generally difficult to have a good low frequency loudspeaker response with small loudspeakers, it is pertinent to ask whether other options are available. One option is to use BWE, with the 'extension' taking part in the auditory system, instead of extending the actual physical bandwidth of the signal. This approach is to make use of the 'missing fundamental' effect: a special case of residue pitch, also known as virtual pitch. We can substitute an $f < f_1$ by a series $kf, k > 2$, to evoke the residue pitch of f, while the loudspeaker does not radiate energy at frequency f. For voice clarity, we try to make the muffled voice more brilliant and clear by three simple algorithms. First of all, we modulate the magnitude of certain frequency components by graphic equalizers [18] to enhance human speech. Second, we use nonlinear process to generate high frequency harmonics. Finally we combine aforementioned two.

2.1 NONLINEAR PROCESSING

In this chapter we describe an efficient nonlinear operation to extend frequency bandwidth. This algorithm is convenient ways for generating harmonics signals with odd or even harmonics. They have their own spectral characteristics and can create different kinds of audio effects. Before explaining the applications of BWE, how the nonlinear processing works and what the characteristics of nonlinear process are should be described [19].

2.1.1 Clipper

A convenient way to generate a harmonics signal with only odd harmonics

is by means of a clipper. The clipper output signal g_c in response to an input f is

$$g_c(t) = \begin{cases} f(t) & if \quad |f(t)| \le l_c \\ l_c & if \quad f(t) > l_c \\ -l_c & if \quad f(t) < -l_c, \end{cases} \tag{1}$$

where l_c is the threshold. The clipper in Fig. 1 demonstrates very good subjective results in the low-frequency psychoacoustic BWE application. This effect due to clipper sounds low-pitched and saturated enough, so the method is applicable to the realization of virtual bass. We can get information from Fig. 2 that only odd harmonics are created by clipper and the fundamental frequency is still preserved. The differences between clipper and rectifier are not only positions of harmonics generated but also preservation of the fundamental frequency. Another disadvantage for a clipper, like a rectifier, cannot control the magnitude of harmonics.

2.1.2 Hyperbolic tangent

Unlike the clipper that is a “hard” clipper, the hyperbolic tangent function shown belongs to a “soft” clipper. Fig. 3 shows the transform of a sine wave 100 Hz on the time and frequency domains by the methods of hyperbolic tangent. We can notice that the waveform modified by the hyperbolic tangent in Fig. 3(a) seems to be compressed. This approach is especially suitable for dialogues but not music, which will be validated in section 2.3. It uses a function that has a gain at low and moderate signal levels, but attenuation at high signal levels. It is different form ordinary compressors because it’s memoryless. That is, it is an instantaneous compressor. During experiments, it appeared that the function where $x(t)$ is the input time signal, and $y(t)$ is the modified output signal by hyperbolic tangent.

$$y(t) = c_1 \tanh(c_2 x(t)) \tag{2}$$

The constant c_1 determines the maximum output level and c_2 determines the gain at low signal levels.

2.2 Virtual bass

With good properties of spectral characteristics, temporal characteristics and inter-modulation distortion [20], we choose the clipper as the method of creating harmonics because of the best low-frequency psychoacoustic performance. Figure 4 shows the whole process of VB realization. There are two paths, the first path is the main structure performing virtual bass, and another path just contains delay. First of all, because of efficiency of running program, we use the method of multistage to execute the up/down-sampling [21] to save evaluation, we chose the up/down-sampling ratio as $M = 16$, and the length of original signal will decrease 16 times after operation. Figure 5 shows that the up/down-sampling process divides into two sections, it is called the interpolated FIR (IFIR) technique [22]. We choose 8 as the first up/down-sampling ratio as well as choose 2 as the second.

In order to avoid frequency aliasing, we must design low pass filters $I(z)$ and $G(z)$. Figure 6 shows how we design the multistage filter. As $I(z)$ is concerned, if the first up/down-sampling ratio is M_1 and the second is M_2, the pass band frequency is determined as $\frac{7}{8}\left(\frac{\pi}{M_1 M_2}\right)$ when the stop band frequency is determined as $\frac{(2M_2 - 1)\pi}{M_1 M_2}$, where π is the half of sampling rate. After we get the frequencies of pass band and stop band, we can design filter on our self by matlab toolbox. One important parameter should be noticed is the filter order, it is determined by the equation as follows.

$$N \approx 2\pi \frac{D(\delta_1, \delta_2)}{\omega_s - \omega_p} \tag{3}$$

Where $D(\delta_{1,}\delta_2)$ is a function of the peak pass-band ripple $\delta_{1,}$ and peak stop ripple δ_2, 2π is sampling rate, ω_s is the stop band frequency, and ω_p is the pass band frequency Form above discussions, we see that the order of $G(z)$ in terms of the specifications δ_1, δ_2, ω_p, and ω_s can be written as

$$N_g = 2\pi \frac{D(0.5\delta_{1,}\delta_2)}{M_1(\omega_s - \omega_p)} \tag{4}$$

The order of $I(z)$

$$N_i = 2\pi \frac{D(0.5\delta_{1,}\delta_2)M_1}{2\pi - (\omega_s + \omega_p)M_1} \tag{5}$$

The number of MPU is approximately

$$\frac{N_g}{2M} + \frac{N_i}{2M_1} = \frac{\pi D(0.5\delta_{1,}\delta_2)}{MM_1(\omega_s - \omega_p)} + \frac{\pi D(0.5\delta_{1,}\delta_2)}{2\pi - (\omega_s + \omega_p)M_1} \tag{6}$$

Next, between the up-sampling with down-sampling process, a band-pass filter should be designed. The filtering signal is applied to create harmonics for virtual bass. The bandwidth becomes 3 kHz after executing the down-sampling process, so the band pass filter order is much less than that without doing down-sampling process. Figure 7 shows that band pass filters (a) and (b) have almost the same performance, however, (a) only need 60 filter order when (b) must need 960 filter taps. This is because (a) was done by down-sampling.

Table 1 shows the comparison between a direct design without up/down-sampling and the multistage design. We can observe that using multistage design is more efficient in running the program.

2.2.1 Timbre Loudness Control

We use clipper, which described in Section 2.1 for creating harmonics after

doing up and down sampling process. Then an adjustable gain control will be used. If this procedure is not performed, the signal modified by clipper is not amplified or attenuated as a desired output. Instead of adjusting the loudness by equal loudness contour, we use timbre loudness control to obtain a suitable spectrum and timbre. It not only controls the loudness but avoids the distortion of timbre. As the equalizer is concerned, it is similar to adjust again control over the whole bandwidth. Now the work we do is the same purpose as the equalizer to design frequency curves which fit with different requirements. Each step is introduced as follows.

First, we use the white noise as the input signal, and pass it along clipper and also create a long bandwidth of harmonics. Next, we try to design a frequency curve in frequency domain, and let the input signal be filtered off the frequency curve. After try and error, if the output sounds like the white noise in loudness and timbre, this frequency curve is the optimal design. Finally, after combination of the first and second path, a high pass filter should be design for avoiding reduction of high frequency components.

Virtual bass can also be performed on a cell phone whose loudspeaker size is much smaller than the common one, but we must redesign the range of band pass filter. The fundamental resonant frequency of a cell phone is almost 1000Hz when the fundamental resonant frequency of ordinary speakers is 200Hz~300Hz approximately. That is why I want to shift the range of band pass filter to 500Hz~1000Hz instead of 50Hz~200Hz. This process is also implemented on automotive audio.

2.3 Voice clarity

Figure 8 shows our structure for implementing a 9 band graphic equalizer using second order IIR filters. The feed forward path is a fixed gain of 0.25, while each

filter band can be multiplied by a variable gain for gain or attenuation. a and b coefficients can be generated for the following second-order transfer function and equivalent input and output difference equations:

$$H(z)=\frac{Y(z)}{X(z)}=\frac{b_0+b_1z^{-1}+b_2z^{-2}}{1-a_1z^{-1}-a_2z^{-2}} \tag{7}$$

In theory, coefficients a_1, a_2 can be found by the relation between the center frequency ω_n and quality factor Q.

$$Q=\frac{\omega_n}{BW}=\frac{1}{2\zeta} \tag{8}$$

where ζ is the damping ratio. After determining the nature frequencies ω_1 and ω_2, the center frequency ω_n, bandwidth BW,and quality factor Q will be found rapidly. Then, we can obtain the coefficients a_1, a_2. Practically, to get the coefficients of the low-pass filters, we use MATLAB filter design toolbox. After determining and setting up the filter type, design method, filter order, and frequency specification, then the coefficients will be found soon.

After describing the theory of graphic equalizer, we try to implement voice clarity by means of it. A simple way performed easily is boosting the amplitude within proper frequency ranges to clarify human voice. Figure 9 shows the frequency response of frequency range and magnitude for boosting. Each solid line indicates the frequency response of each filter band in different frequency ranges, and the dashed line represents the sum of total frequency response.

Hyperbolic tangent has been described in Section 2.2 and it is suitable for high frequency extension and dialogues processing. Similar to graphic equalizer, a simple way is proposed to realize voice clarity. Figure 10(a) shows the structure. Because the magnitude of bass or low frequency is usually much louder than the one of high frequency, let original signal pass through a high pass filter is our first step. Next,

use hyperbolic tangent to enhance voice or high frequency component. After gain-adjusted, add the original music from the other path and the output is done.

In this section there is no innovation proposed, we have aforementioned methods combined to achieve voice clarity. Figure 10(b) shows the structure.

3 INTRODUCTION OF UP/DOWNMIX PROCESSING

In recent years, computer, communication, and consumer, generally referred to as the 3C industries are rapidly advancing. The appearance of the digital versatile disk (DVD) and the super audio CD (SACD) has provided high quality audio and video presentations. Also, the rapidly-developed third-generation (3G) handsets equipped with dual-loudspeaker would have a chance to deliver high quality audio reproduction. Using multichannel audio reproduction technology, consumers are now able to immerse themselves seamlessly with multimedia in a theater-like environment. In multichannel audio reproduction, upmix and downmix processing plays an important role in many audio applications, where the number of channels of either the audio content or the reproducing loudspeakers is limited In order to support the compatibility with two-channel stereo signals, the upmix processing, having been studied extensively, is employed to creating additional channels based on original audio channels [23~27]. Since five channels have been shown to be sufficient for simulating ambience circumstance [25], it is focused on translating the two-channel signals into the multichannel 5.1 reproduction format in this chapter. Two general strategies for upmix processing including the direct-ambient approach and the 'in-the-band' approach have been proposed [28]. The direct-ambient approach describes that the front speakers refer to position the direct sound images and deliver dialog, whereas the rear surround speakers refer to reproduce only diffuse and background sound field giving rise to a sense of ambience and envelopment. The

‘in-the-band’ approach suggests that all loudspeakers are required to produce a sound field in the foreground as if the listener were surrounded by sources. Furthermore, the fact that upmix processing creates additional channels on the basis of the stereo inputs can be achieved by using two strategies. One approach attempts to extract the “de-correlated” part of the original audio signals, whereas another approach attempts to produce the additional ambient reverberation that simulates the diffuse sound field in the background. There are two methods of the first category including the passive surround decoder method [26] and reverberation based method. And the room response simulator mentioned before is employed to create the spaciousness and ambience. Contrary to the upmix processing, the downmix processing refers to reduce the number of channels due to practical reasons such as availability of loudspeakers. In this thesis, it is focused on remixing the 5.1 audio inputs into two-channel signals since the rendering loudspeakers are predominantly stereo in 3C products. For this purpose, downmix can be accomplished by simple mixing or the head related transfer function (HRTF) filtering, as in Sound Retrieval System (SRS) 3D stereo sound system [29]. HRTF [30] is a mathematical model representing the propagation process from a sound source to the human ears and contains spatial cues such as propagation delay and diffraction effects due to the head, ears, and even the torso. This allows us to create a directional impression by properly synthesizing HRTFs. As described, upmix refers to creating additional channels of signals based on original audio channels, whereas downmix refers to remixing multichannel audio inputs into a decreased number of channels. However, it is noted that if the audio inputs and the reproducing loudspeakers are both of two-channel stereo configuration, then upmix could be concatenated with downmix to simulate a multichannel environment.

3.1 Upmix algorithm

In this section, five upmix algorithms including the passive surround decoder method, the adaptive panning method, the LMS-based method, the PCA-based method, and the artificial room simulator method are introduced. These methods differ in how to generate the additional channels based on original audio channels. In general, the center (C) channel corresponds to the most correlated portion between the front right (FR) and the front left (FL) channels. A 128-tap FIR band-pass filter with cut-off frequencies 100 Hz and 4 kHz is employed to emphasize voice and dialog for center channel. The rear left (RL) and the rear right (RR) channels are intended to provide ambience and environment affects. Thus, a 15 ms delay is added to the rear channels to comply with the precedence effect. The feature of high-frequency absorption can be simulated by filtering the rear channels with a 7 kHz cut-off, 128-tap FIR low-pass filter. In addition, the rear channels are also 180-degree out-of-phase with one another, which helps spaciousness of the ambient field [31]. The low frequency enhancement (LFE) channel is derived from the center channel before band-pass filtering. A 128-tap FIR low-pass filter is used to retain the signals below 120 Hz for the LFE channel. The general architecture of the direct-ambient upmix approach for creating the additional channels is shown in Fig. 11.

3.1.1 The passive surround decoder method

The first approach employed in this study attempts to emulate an early passive version of the Dolby Surround Decoder [26] as shown in Fig. 12. The center channel results from the average of the original stereo channels, whereas the rear surround signals result from the difference. As above-stated, the center channel is band-pass filtered to focus on the voice signal and the rear surround channels are delayed, low-pass filtered and 180-degree out-of-phase with one another. The LFE channel is generated by filtering the center channel by the 120 Hz low-pass filter.

3.1.2 Reverberation based method

The reverb has room modes such as church, small club, living room or gymnasium. We can select the mode of Reverb filter to produce the effect of the true environment. The algorithm of reverb can make the sound have more surround effect. There are many important properties about the room response needed to be considerer in the design of efficient reverberators and we will discuss them as follow.

- Echo Density

In the time domain, the echo density of a room response was defined as the number of echoes reaching the listener per second.

$$N_t = \frac{4\pi(ct)^3}{3V}, \tag{9}$$

where N_t is the number of echoes, t is the time (in s), ct is the radius of the sphere (in m) centered at the listener, and V is the volume of the room (in m^3). As differentiating with respect to t, we obtain that the density of echoes is proportional to the square of time:

$$\frac{dN_t}{dt} = \frac{4\pi c^3}{V} t^2. \tag{10}$$

- Modal Density

The normal modes of a room are the frequencies that are naturally amplified by the room. The number of normal modes N_t below frequency f is nearly independent of the room shape and is given as follow:

$$N_f = \frac{4\pi V}{c^3} f^3 + \frac{\pi S}{4c^2} f^2 + \frac{L}{8c} f, \tag{11}$$

where c is the speed of sound (in m/s), S is the area of all walls (in m^2), and L is the sum of all edge length of the room (in m). The modal density was defined as the number of modes per Hertz.

$$\frac{dN_f}{df} \approx \frac{4\pi V}{c^3} f^2, \tag{12}$$

Thus, the modal density of a room response grows proportionally to the square of the frequency.

- Reverberation Time

The room effect is often characterized by its reverberation time, a concept first established by Sabine in 1990. The reverberation time is proportional to the volume of the room and inversely proportional to the amount of sound absorption of the walls, floor and ceiling of the room. The Sabine's empirical formula estimating the reverberation time lists as follows:

$$T_{60} = \frac{0.163 \cdot V}{A} = \frac{0.163 \cdot V}{\sum_i a_i S_i}, \tag{13}$$

where T_{60} is the time for the sound pressure to decay 60 dB, V is the volume of the room (in m^3), S_i and a_i are the surface of a material employed in the room and the associated absorption coefficient, and the total absorption of material is A. Since most materials of surface in a room are more absorptive at high frequencies, the reverberation time of a room is also decreases as the frequency increases. The reverberation time is used for estimating the degree of sound absorption in a room.

- Energy Decay Curve (EDC) and Energy Decay Relief (EDR)

The method to determine the reverberation time of a measured room is finding the time when the associated sound pressure attenuate 60 dB in the plot of the EDC, Schoroeder proposed in 1965. He suggested integrating the impulse response of the room to get the room's energy decay curve.

$$EDC(t) = \frac{\int_t^\infty h^2(\tau) d\tau}{\int_t^\infty h^2(\tau) d\tau}, \tag{14}$$

where $h(\tau)$ is the impulse response of the room. Later, Jot proposed a variation of

the EDC to help visualize the frequency dependent natural of reverberation called the energy decay relief $EDR(t,\omega)$. The EDR represents the reverberation decay as a function of time and frequency in a 3D plot. To compute it, we divide the impulse response into multiple frequency band and compute Schoroeder;s integral for each band.

- Modeling Early Reflection

A room response from a source to a listener can be obtained by solving the wave equation also known as the Helmholtz equation. However, it can seldom be preformed in an analytic form and is more complex in solving. Therefore, the solution must be approximated and there are three different approaches in computational modeling of room based on acoustics [32]. The ray-based methods, including the ray-tracing and the image-source method, are the most often used modeling techniques. With the assumption of the wavelength of sound is small compared to the area of surface in the room and large compared to the roughness of surface, all phenomena due to the wave nature, such as diffraction and interference, are ignored. The image-source method examines the effects of an acoustic source in a room with corresponding sources located in image rooms with reflecting boundaries. Each of the infinite sources will produce attenuated, filtered and delayed version of the original acoustic input. The total effects can be summed to produce a transfer function or a FIR filter.

- Modeling Late Reverberation

There are two approaches to model late reverberation, the FIR-based and IIR-based methods. Implementing convolution using the direct form FIR filter is extremely inefficient when the filter size is large. Typical room responses are several seconds long, which at a 44.1 kHz sampling rate would translate to a huge number of points filter. One method to deal with the large size FIR filter is using an

algorithm based in the Fast Fourier Transform (FFT) block convolution [33]. The second method is try to model the late reverberation of a room based on some IIR-filters, comb and all-pass filters, Schoroeder proposed first in the early 1960's, or a mixture of them. The details of comb filter and all-pass filter will be discussed in the next section.

- Comb Filter

The block diagram of comb filter shown in Fig. 13 consists of a single delay line of m samples with a feedback loop containing an attenuation gain g. The z-transform of the comb filter is given by:

$$H(z) = \frac{z^{-m}}{1 - gz^{-m}}. \tag{15}$$

Note that to achieve stability, g must be less than unity. The time response of this filter is an exponentially decaying sequence of impulse spaced m samples apart. This is good for modeling reverberation because real room have a reverberation tail decaying somewhat exponentially. However, the echo density is really low, causing a "fluttering" sound on transient input. The pole-zero map of the comb filter shows that a delay line of m samples creates a total of m poles equally spaced inside the unit circle when it is stable. Half of the poles are located between 0 Hz and the Nyquist frequency $f = f_s / 2$ Hz, where f_s is the sampling frequency. That is why the frequency response has m distinct frequency peaks giving a "metallic" sound to the reverberation tail. We perceive this sound as being metallic due to hearing the few decaying tones that correspond to the peaks in the frequency response.

- All-pass Filter

Because the poor performance of frequency response of a comb filter, Schroeder modified to provide a flat frequency response by mixing the input signal and the comb filter output as shown in Fig. 14. The resulting filter is called an allpass filter

because its frequency response has unit magnitude for all frequencies. The z-transform of the all-pass filter is given by:

$$H(z) = \frac{z^{-m} - g}{1 - gz^{-m}}. \tag{16}$$

The poles of the all-pass filter are thus the same as for the comb filter, but the all-pass filter now has zeros at the conjugate reciprocal locations.

And the response of an all-pass filter sounds quite similar to the comb filter, tending to create timbre coloration.

■ Nested All-pass Filter

To achieve a more natural-sounding reverberation network, it would be desirable to combine the unit filters to produce a buildup of echoes, as it would occur in real rooms. One solution to produce more echoes is cascading multiple all-pass filters which Schroeder had experimented with reverberators consisting of 5 all-pass filters in series. Schroeder noted that these reverberators were indistinguishable from real rooms in terms of coloration, which may be true with stationary input signals, but other authors have found that series all-pass filters are extremely susceptible to tonal coloration, especially with impulsive inputs. Gardner proposed reverberators based on a “nested” all-pass filter, where the delay of an all-pass filter is replaced by a series connection of a delay and another all-pass filter. The block diagram and its impulse response are shown in Fig. 15(a), where the all-pass delay is replaced with a system function $N(z)$, which is all-pass. Then the transfer function of this from is written:

$$H(z) = \frac{N(z) - g_1}{1 - g_1 N(z)}. \tag{17}$$

The advantage of using a nested all-pass filter can be seen in the impulse response in Fig. 15(b). Echoes created by the inner all-pass filter are recirculated to itself via the outer feedback path. Thus the echo density of a nested all-pass filter increases with time, as in real rooms.

3.2 Downmix algorithm

The creation of DVD and SACD causing a revival of multichannel audio has carried out the high quality audio performance. However, many applications such as personal computer multimedia, portable audio products, TVs and cell phones are equipped with only stereo loudspeakers. Thus, downmix processing is necessary to downmix a multichannel content, e.g., 5.1 into two channels. Two downmix techniques will be presented as follow.

3.2.1 The standard downmix method

The method suggested in the ITU standard [34] refers to mix the multichannel signals with simple gain adjustment. The architecture of the standard downmix method is shown in Fig. 16. In this method, the center channel is attenuated by 0.71 (or 3 dB) and mixed into the front channels. Similarly, the rear left and the rear right surround channels are attenuated by 0.71 and mixed into the front left and the front right channels, respectively. That is,

$$\begin{aligned} L &= FL + 0.71 \times C + 0.71 \times RL \\ R &= FR + 0.71 \times C + 0.71 \times RR \end{aligned} . \tag{18}$$

Nevertheless, depending on the rendering loudspeaker system, the LFE channel can be mixed into the front channels as an option.

3.2.2 The HRTF-based downmix method

In addition to the aforementioned standard downmix method, the approach employing the HRTF technique is included in this thesis. The HRTF technique allows us to create a directional impression so as to enhance to the multichannel reproduction in the downmix processing. In the HRTF-based method, no special processing is applied to the front left and the front right channels. The center, the rear left, and the rear right channels are filtered by the corresponding HRTFs at 0°, $+110^\circ$, and

-110°, respectively, before mixing with the front channels. The HRTF database implemented by using 128-tap FIR filters is from the website of the MIT media lab [30]. Thus, the front right channel, front left channel, rear right channel and rear left channel can felt more directional.

3.3 Two-channel inputs for automotive audio

In traditional automotive audio, the left-input signals are fed to both front-left and rear-left loudspeakers, and the right-input signals are fed to both front-right and rear-right loudspeakers. Balance of the left and right as well as the front and the rear can usually be adjusted. The problem with this approach is that the front and rear channels are too correlated to create natural-sounding surround effects. The paper seeks to develop upmixing algorithms for extending two-channel input to four channels. Upmixing can generally be achieved by two categories of approaches. One approach is decorrelation-based methods, e.g., Prologic II and Logic 7, etc. Another approach is reverberation-based method that is found to be very effective in producing sense of space, especially for small space [35]. In a previous subjective listening test [36], the reverberation-based methods outperformed the decorrelation-based methods in ambient surround effects. Thus, only the reverberation-based upmixing method is adopted in the following discussion.

Here developed as an alternative solution to the problem of automotive surround audio. Figure 18 shows the block diagram of this method, in which concatenated upmixing and down mixing processing is required. In the study, weightings (0.65) and delay (20 ms) are used. The upmix module is described here, where two-channel input signals are extended to four channels by the reverberation-based upmixing algorithm and then inverse filtered to produce the outputs. An artificial reverberator is employed to produce the rear surround channels. The artificial

reverberator is constructed from 3 parallel comb filters shown in Fig. 17(a) and a 3-layered nested-allpass filter shown in Fig. 17(b). The difference between the left and right input signals is mixed into the rear channel to enhance ambience. The rear-left and rear-right channels are made 180° out of phase.

With the upmixed signals, downmixing can be done by two methods. One is only done by standard weighting and summation to produce the two-channel outputs. The other one is done by HRTF downmixing, which is mentioned before.

3.4 5.1-channel inputs for automotive audio

Another category of automotive surround processors that accepts 5.1 input signals from Dolby Digital or DTS decoder in DVD players will be presented in this section.

The strategy here is developed for inputs in 5.1 formats, as depicted in the block diagram of Fig. 19. In the method, the center channel is first mixed into the front two channels and then the ipsi-lateral channels are summed to produce the two frontal channels. Next, the frontal channels are weighted and delayed to produce the rear channels. The downmixing methods are the same as the above method. When the downmix processing is done, the surround channels are produced by the weighting and delay of front channels.

4 ADAPTIVE AUDIO GAIN CONTROLLER BASED ON NOISE LEVEL ESTIMATION

Noises resulting from the engine, panel vibration, tire, wind, pass-by traffic, air conditioning, etc., could significantly degrade the music listening quality in a car. This paper proposes a new system that makes use of a Noise Level Estimator (NLE) in tandem with s Dynamic Range Controller (DRC) to adaptively adjust the gain of an automotive audio system. A microphone is required in the NLE as the senor to pick

up music signals corrupted with cabin noise. The background noise level is estimated adaptively using the Least-Mean-Squares (LMS) algorithm. The *a priori* Signal-to-Noise Ratio (SNR) is calculated based on the noise level estimated above. From the SNR, the gain of the audio input can be adjusted dynamically, with the aid of a static curve. The system has been implemented by using a Digital Signal Processor (DSP) on a real car. Results obtained from simulations and experiments reveal that the proposed system is capable of regulating the audio volume on the fly, in response to the noise in the car cabin.

4.1 Noise level estimation by least mean square method

System identification is the procedure of analyzing an unknown system. The well-known method to achieve the identification processing is the LMS algorithm [7]. The system structure is shown in Fig. 20, where $x(n)$ is the input signal and $x_p(n)$ is the desired signal. The desired signal can be determined by the optimal coefficient $w_s(n)$, which is obtained by minimizing the error signal $e(n)$. Basically, the system learns from its environment is designated as an adaptive filter where the filter coefficients are updated according to

$$\mathbf{w}_s(n+1) = \mathbf{w}_s(n) + \mu_s e(n)\mathbf{x}(n) \quad , \tag{19}$$

where

$$\mathbf{w}_s(n) = [w(1)\ w(2)\ \ldots\ w(N)]^T \tag{20}$$

is the filter coefficients vector of dimension $N \times 1$.

$$\mathbf{x}(n) = [x(n)\ x(n-1) \ldots x(n-N+1)]^T \tag{21}$$

is the input signal vector of dimension $N \times 1$.

And μ_s is the step size. The stability of such a closed-loop system is governed by the adaptation parameter and it should satisfy the condition

$$0 < \mu_s < \frac{2}{L \cdot P_x}, \tag{22}$$

where L is filter length and P_x is the total power of $x(n)$. The total power of $x(n)$ is the sum of mean-square value of the input signal. When μ_s is small, it takes more time to converge to a minimum error, and vice versa.

Applied in a noisy condition, system identification is a pre-processing for NLE. As the unknown plant is determined, the noise can be estimated from the difference between noisy path and noise-free path. See Fig. 20, $x(n)$ is the input signal, $x_p(n)$ is the signal through a plant and receive from a microphone. $v(n)$ is the background noise. The above system can be written as

$$d(n) = x_p(n) + v(n). \tag{23}$$

The FIR estimator for the system is defined by

$$y(n) = \mathbf{x}(n)\mathbf{w}_s(n). \tag{24}$$

According to the processing of system ID the optimum parameters of the unknown plant can be determined by minimizing the Mean-Square-Error (MSE).

$$\min E[e_{ID}^{\ 2}(n)], \tag{25}$$

where $E[\cdot]$ denotes the expectation operator. And $e_{ID}(n)$ is defined as follow

$$e_{ID}(n) = x_p(n) - y(n) = x_p(n) - \mathbf{x}(n)\mathbf{w}_s(n). \tag{26}$$

In the case, the estimation error $e_{NLE}(n)$ is expressed as the difference between the measured and the predicted system output,

$$e_{NLE}(n) = d(n) - y(n) = x_p(n) + v(n) - \mathbf{x}(n)\mathbf{w}_s(n), \tag{27}$$

The system setup is illustrated in Fig. 20. Here, $v(n)$ and $x_p(n)$ are assumed to be uncorrelated. When the signal $x_p(n)$ is determined and equal to the output $y(n)$ then $e_{NLE}(n)$ is equal to $v(n)$.

4.2 Dynamic range control

DRC of audio signal is used in many applications to match the dynamic behavior of the audio signal to different requirements. While recording, DRC protects the AD convector from overload or it is used in the signal path to optimally use the full amplitude range of a recording system. When reproducing music and speech in a car, the dynamics have to match the noise characteristic inside a car. A DRC is an automatic gain control device which modifies the dynamic range without introducing perceptible distortion. Fig. 21 shows a block diagram of DRC system. After measuring the level of input signal *x*, the output signal *y* is affected by multiplying the delayed input signal by a factor $g(n)$ according to

$$y(n) = g(n) \cdot x(n - D), \tag{28}$$

where D is the delay sample for non-process path and $g(n)$ is a gain factor that obtained according to the input level. Level measurement plays an important role in DRC. The rapidity of DRC depends also on the measurement of RMS values [10]. The RMS measurement is shown in Fig. 22. Uses the square of the input and performs averaging with a first-order low-pass filter. The difference equation is given by

$$x_{RMS}(n) = (1 - \tau) \cdot x_{RMS}(n - 1) + \tau \cdot x^2(n), \tag{29}$$

where $x_{RMS}(n)$ is signal through the RMS measurement processing and τ is the average coefficient. The transfer function is

$$H(z) = \frac{\tau}{1 - (1 - \tau) z^{-1}}. \tag{30}$$

The system also serves to smooth the gain multiplier by using the attack coefficient and release coefficient. The attack coefficient AT (attack time) and release coefficient RT (release time) is obtained by comparing the input signal and the previous sample. Then the system determines whether the control factor is in the

attack or release status. If the input signal is lager than the previous signal, then system gives the attack coefficient AT. If the input signal is smaller than the previous signal, then system gives the release coefficient RT.

The relationship between input level and weighting level is defined by static curve. In this paper, the output level and the weighting level are given as functions of the input SNR level g[dB] = f(SNR[dB]). Fig. 23 shows a static curve which varies with the SNR. According to the static curve, the limiter threshold is 6 dB. The output gain is limited when the SNR level exceeds the limiter threshold. All SNR levels less than this threshold lead to a constant output gain 6 dB. The SNR between 5~25 dB represents an amplifier, and has two slopes. The slope between 5 dB SNR to 20 dB SNR is 0.2. The slope between 20 dB SNR to 30 dB SNR is 0.3. Both the two parts are compressor curves. The SNR exceeding 30 dB leads to a constant gain 0 dB.

4.3 Integration of NLE and DRC modules

The two systems mentioned above have their own specific applications. This paper is focusing on how to improve the listening quality in a car environment. We combined NLE system and DRC system to deal with the noisy condition in a car. The system block diagram is shown in Fig. 24. Take the NLE system as first step, the optimal parameter of the adaptive filter is obtained from eq. (19). Then according to eq. (25), eq. (26) and (27) the background noise level can be accurately estimated from a noisy signal. The signal then goes through RMS level measurement and turns into x_{RMS} by eq. (29). Because the purpose is trying to adaptively adjust the output signal gain according to background noise, the signal to noise ratio (SNR) is an important factor. Use the power of background noise level and the power of signal level to calculate *a priori* SNR, where *a priori* SNR is given by

$$\zeta = \frac{\left| x_p^{\,2} \right|}{\left| v^2 \right|}, \tag{31}$$

where x_p is the signal through plant and v is background noise.

As mentioned before, the static curve needs to be designed in advance. Based on *a priori* SNR and static curve, the output gain mapping can be determined.

4.4 System simulation and experimental investigation

Simulations and experiments are undertaken to validate the NLE and DRC modules proposed in the paper.

A. Simulations

We evaluated the proposed algorithm by performing a system simulation of the adaptive gain controller system. As the proposed processing mentioned before, the adaptive filter is used to track the plant when the NLE system is working. According to the NLE system structure shown in Fig. 20, the filter coefficients are adaptively calculated from eq. (19), and the step size is equal to 0.45. From eq. (19), (25) and eq. (26) the optimal parameter is determined when the error is converging.

In Fig. 20, the program input $x(n)$ is an 8-second music excerpt and $v(n)$ is an 8-second background noise. The background noise is a level varying whitenoise. When the unknown plant is determined, the background noise can be calculated by (27). See Fig. 25, the upper row is the original background noise and the lower row is the estimated background noise. After the background noise is estimated, the system then calculates the *a priori* SNR by (30). Fig. 26 shows the SNR curve, this is calculated by the signal and the background noise which is varying in 3 different levels. From Fig. 26, the SNR fluctuates between 12 dB to 31 dB. There is an obvious notch from the 2nd to the 6th second. According to the purposed algorithm, the output gain curve should obtain a higher gain when the SNR curve is falling to a

notch. The relationship between input SNR level and gain level is defined by a static curve. The static curve has described in section III. With the aid of the static curve and the calculated SNR curve, the output gain can be obtained. Fig. 27 shows the output gain curve. When the SNR is small, the system gets a higher gain. When the SNR is high, the system gets a lower gain.

B. Experiments

Fig. 28 shows the experimental arrangement. Experiments were conducted in an Opel Vectra 2-liter sedan equipped with a multichannel audio decoder, and four loudspeakers (two mounted in the lower panel of the front door and two behind the back seats). In this section, the adaptive gain controller based on one-microphone noise level estimation is examined. The algorithms were implemented on the platform of a fixed-point DSP, ADI BF-533, of Analog Device semi-conductor. The GRAS 40AC microphone with GRAS 26AC preamplifier was used for receiving the signal and the background noise. The position of the microphone is located at the center of the car.

The experiments were implemented by the following process. We turned on the system and microphone first. Through the DSP board, the program music was played form the right channel. With the ambient noise and the signal, the microphone picked up the noisy signal. The NLE system dealt with the noisy signal. As soon as the adaptive filter approximated the plant, the background noise level can be estimated. After the noise level is estimated, the system would output gains for the input signal to maintain the SNR. There are two cases in this experiment. Case 1 used the ambient noise in a moving car. Case 2 used the level varying whitenoise. Both the noises were played from the left channel. Fig. 29 shows the experimental result of case 1. Fig. 30 shows the result of case 2. The upper row is the waveform when the system is off. The lower row is the waveform when the system is on. In

case 1, the output signal changes moderate because the noise does not have clear level changing. In case 2, the result shows the output signal has obvious level changing with the level varying whitenoise.

5 CONCLUSIONS

In this study, we have proposed an adaptive gain control system based on one-microphone noise level estimation. In this system, we select single channel music and a background noise recorded from a moving car to be the test signal. When system ID, the unknown plant can be accurately tracked by LMS algorithm. The background noise level is then obtained from NLE system. Referring to the theory of DRC, we propose a static curve which uses SNR to determine the output gain.

We have evaluated the proposed algorithm by performing a system simulation, DSP implementation and experiment of the adaptive gain control system. The experimental results show that the system can dynamically adjust the audio gain when the background noise is varying.

REFERENCE

[1] H. Drucker, "Speech Processing in a High Ambient Noise Environment," *IEEE Trans. Audio and Electroacoustics*, vol. 16, no. 2, pp. 165-168, 1968.

[2] M. Heckmann, F. Berthommier and K. Kroschel, "Noise Adaptive Stream Weighting in Audio-Visual Speech Recognition," *EURASIP. Applied Signal Processing*, vol. 11, pp. 1260-1273, 2002.

[3] D. E. Tsoukalas, J. N. Mourjopoulos and G. Kokkinakis, "Speech Enhancement Based on Audible Noise Suppression," *IEEE Trans. Speech and Audio Processing*, vol.

5, no. 6, pp. 497-514, 1997.

[4] B. C. J. Moore, B. R. Glasberg and M. A. Stone, “Optimization of a slow-acting automatic gain control system for use in hearing aids,” *British Journal of Audiology*, vol. 25, no. 3, pp. 171-182, 1991.

[5] S. Haykin, *Adaptive Filter Theory*, Englewood Cliffs, NJ: Prentice-Hall, 2002.

[6] S. Haykin, “Adaptive Filters,” IEEE Signal Processing Magazine, vol. 16, pp. 20.

[7] N. Kalouptsidis and S. Theodoridis, *Adaptive System Identification and Signal Processing Algorithm*, Englewood Cliffs, NJ: Prentice-Hall, 1993.

[8] A. K. Pradhan, A. Routray, and A. Basak, “Power System Frequency Estimation Using Least Mean Square Technique,” *IEEE Trans. Power Delivery*, vol. 20, no. 3, pp. 1812-1816, 2005.

[9] A. Feuer and E. Weinstein, “Convergence analysis of LMS filters with uncorrelated Gaussian data,” *IEEE Trans. Acoust., Speech, Signal Processing*, vol. 33, no. 1, pp. 222–229, 1985.

[10] G. W. McNally, “Dynamic Range Control of Digital Audio Signals,” *J. Audio Eng. Soc.*, Vo1.32, no 5, pp. 316-327, 1984.

[11] A. T. Schneider and J. V. Hanson, “An Adaptive Dynamic Range Controller for Digital Audio,” *IEEE Pacific Rim Conference on Communication, Computers and Signal Processing*, 1991.

[12] M. H. Hayes, Statistical Digital Signal Processing and Modeling, New York: Wiley, 1996.

[13] U. Zolzer, *Digital Audio Signal Processing*, New York: Wiley, 1995.

[14] E. Larsen and R. M. Aarts, and O.Ouweltjes. “A unified approach to low- and high-frequency bandwidth.” the 115th AES convention, New York, Audio Engineering Society, 2003.

[15] M. R. Bai and W. C. Lin, “Synthesis and Implementation of Virtual Bass

System with a Phase-Vocoder Approach," *J. Audio Eng. Soc.* vol. 54, pp.1077-1091, 2006.

[16] T. H. Andersen and K. Jensen, "Importance and Representation of Phase in the Sinusoidal Model," *J. Audio Eng. Soc*., vol. 52, no.11, pp.1157-1169, 2004.

[17] R. E. Crochiere and L. R. Rabiner, *Multirate Digital Signal Processing*. Prentice-Hall, Englewood Cliffs, NJ, 1983.

[18] J. Tomarakos, D. Ledger, *Using The Low-Const, High Performance ADSP-21065L Digital Signal Processor For Digital Audio Applications*, 1998.

[19] E. Larsen, R. M. Aarts and M. Danessis, "Efficient high frequency bandwidth extension of music high frequency bandwidth extension of music and speech," the 112th AES convention, Munich, Germany, May 2002, 10-13.

[20] E. Larsen and R. M. Aarts, *Audio Bandwidth Extension*, John Wiley, West Sussex, England, 2004.

[21] P. P. Vaidyanathan, *Multirate Systems and Filter Banks*, Prentice-Hall, Englewood Cliffs, NJ, 1993.

[22] A. V. Oppenheim and R.W. Schafer, *Discrete-Time Signal Processing*. Prentice-Hall, Englewood Cliffs, NJ, 1999.

[23] Dolby Laboratory, Dolby Surround Pro Logic II decoder Principles of Operation. (http://www.dolby.com/resources/tech_library/index.cfm)

[24] SRS Labs, Circle Surround White Paper. (http://www.srslabs.com/reflibrary.asp)

[25] G. Theile, 1991, *Proc*. 10th *AES Conf. on Image and Audio*, pp.147-162. DTV Sound System: How Many Channels?

[26] Dolby Laboratory, Dolby Surround Pro Logic decoder Principles of Operation, (http://www.dolby.com/resources/tech_library/index.cfm)

[27] M. R. Bai and G. Bai, 2006, *J. Audio Eng. Soc*. Optimal Design and Synthesis of Reverberators with a Fuzzy User Interface for Spatial Audio.

[28] S. K. Zielinski and F. Rumsey, 2003, *J. Audio Eng. Soc*., 51, No. 9. Effects of Down-Mix Algorithms on Quality of Surround Sound

[29] S. Gajjar, 1998, *IEEE Colloquium on Audio and Music Technology*: The Challenge of Creative DSP, London, pp. 15/1-15/7. A 3D Stereo Sound System.

[30] B. Gardner and K. Martin, 1994, MIT Media Lab. HRTF Measurements of KEMAR Dummy-Head Microphone. (http://sound .media.mit.edu/KEMAR.html)

[31] U. Zolzer, 2002, *DAFX, Digital Audio Effects*, John Wiley & Sons.

[32] Savioja, L., 1999, "Modeling Techniques for Virtual Acoustics," Doctorate Thesis, Espoo, Finland.

[33] Oppenheim A. V., and Schafer, R. W., "Discrete-Time Signal Processing," Prentice-Hall, New Jersey.

[34] ITR-R Rec. BS.775-1, 1992-1994, *International Telecommunications Union*, Geneva, Switzerland. Multi-Channel Stereophonic Sound System with or without Accompanying Picture.

[35] M. R. Bai and G. Bai, "Optimal Design and Synthesis of Reverberators with a Fuzzy User Interface for Spatial Audio," *J. Audio. Eng. Soc.*, vol. 59, pp. 812–825 (2005).

[36] Mingsian R. Bai and Geng-Yu Shih, "Upmixing and Downmixing Two-channel Stereo Audio for Consumer Electronics," submitted to *IEEE Trans. Consumer Electron.* (2007).

Table 1 Comparison between direct design and Multistage design

	Direct design	Multistage design			
		G(z)	*I(z)*	BPF	Total
Filter order	960	96	46	60	344
MPU	960	6	5.75	60	83.5
APU	959	12	11.5	59	106

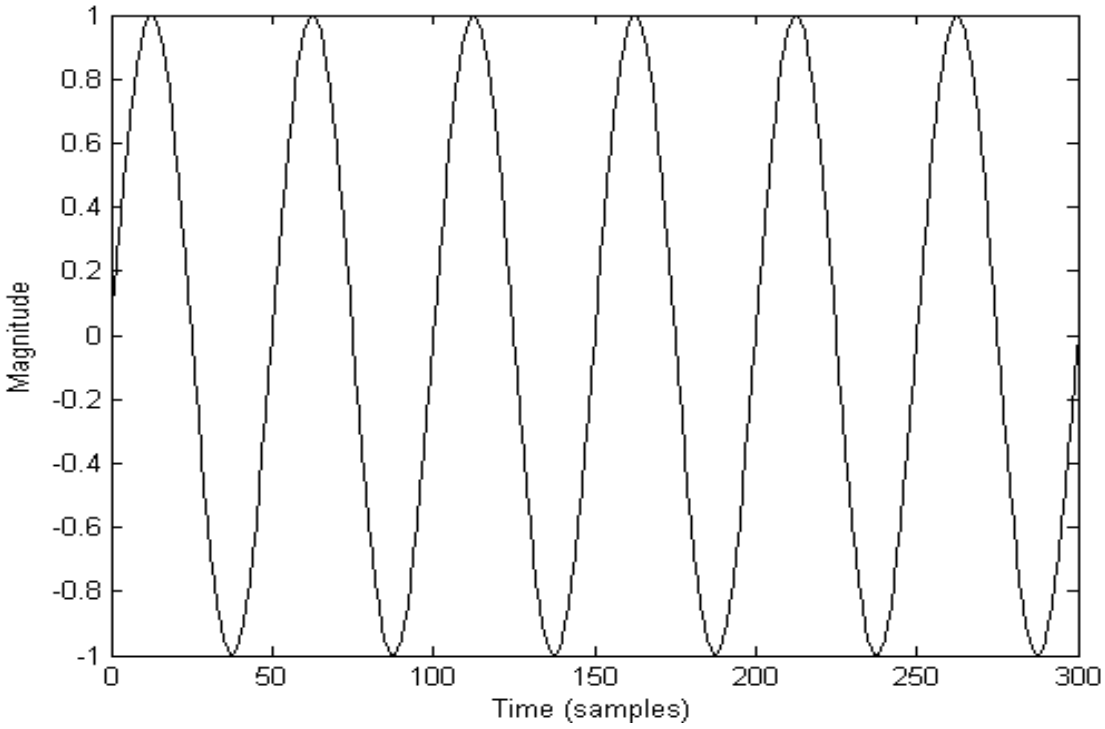

(a)

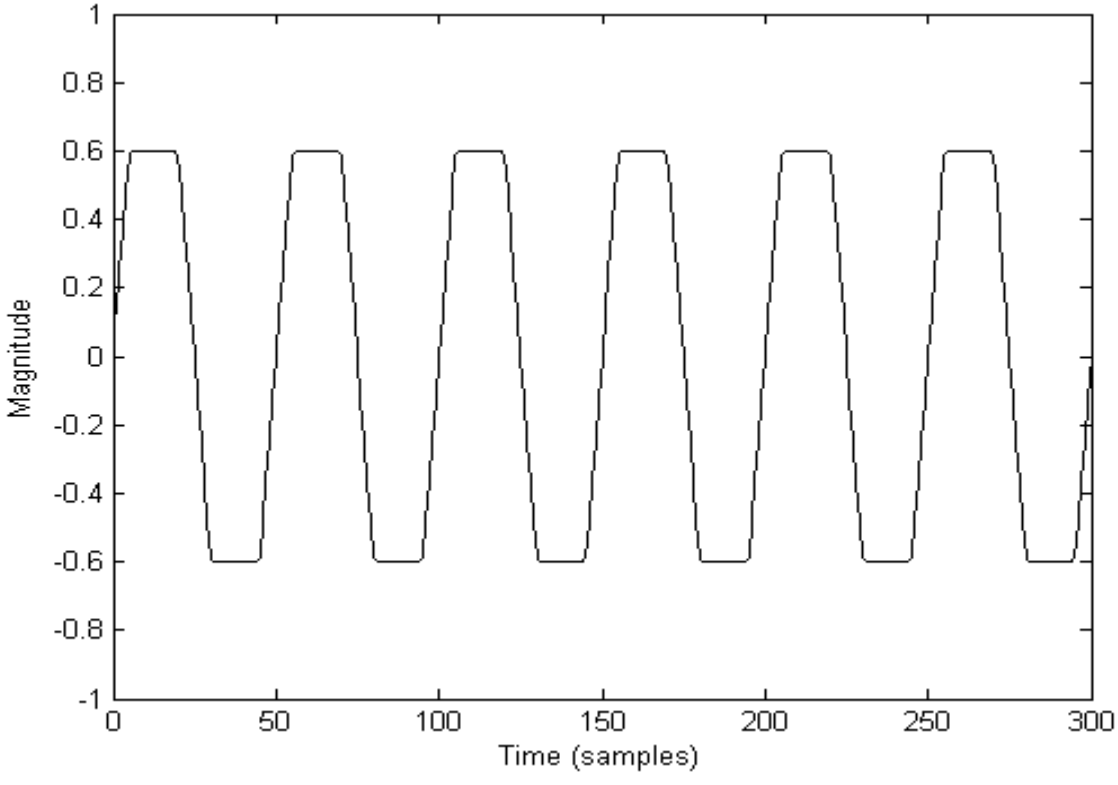

(b)

Fig. 1 The waveforms of a pure-tone (a) and its truncated signal by a clipper (b).

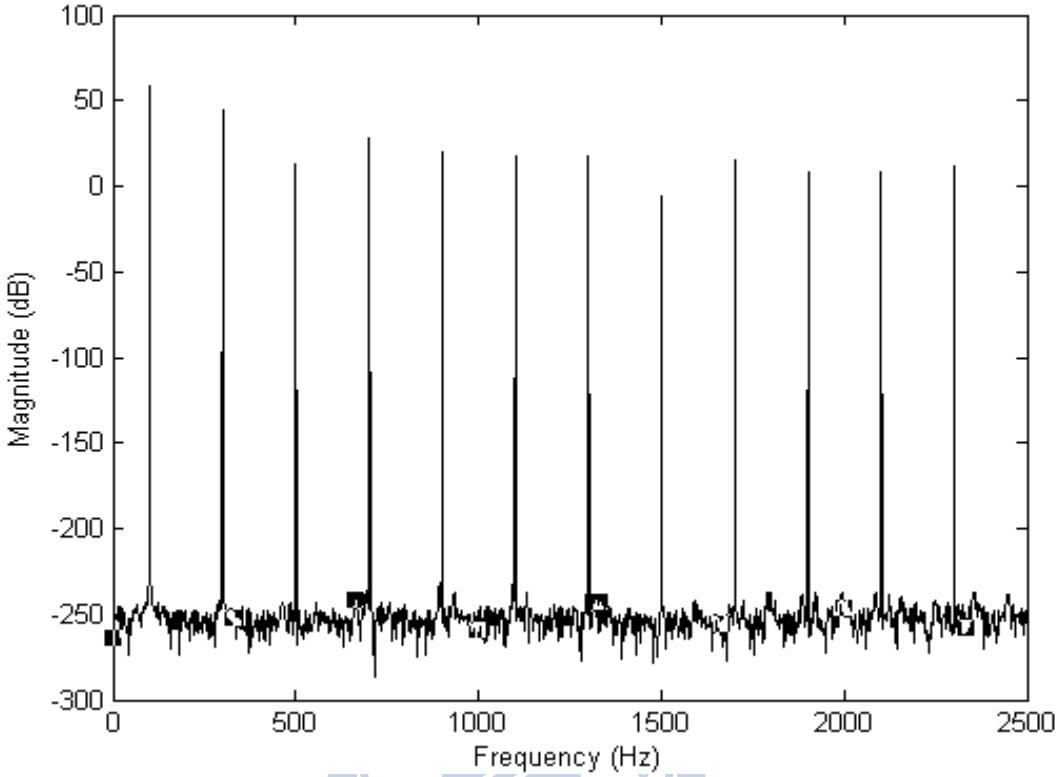

Fig. 2 The frequency spectrum of only odd harmonics generated by a clipper using a sine wave 100Hz.

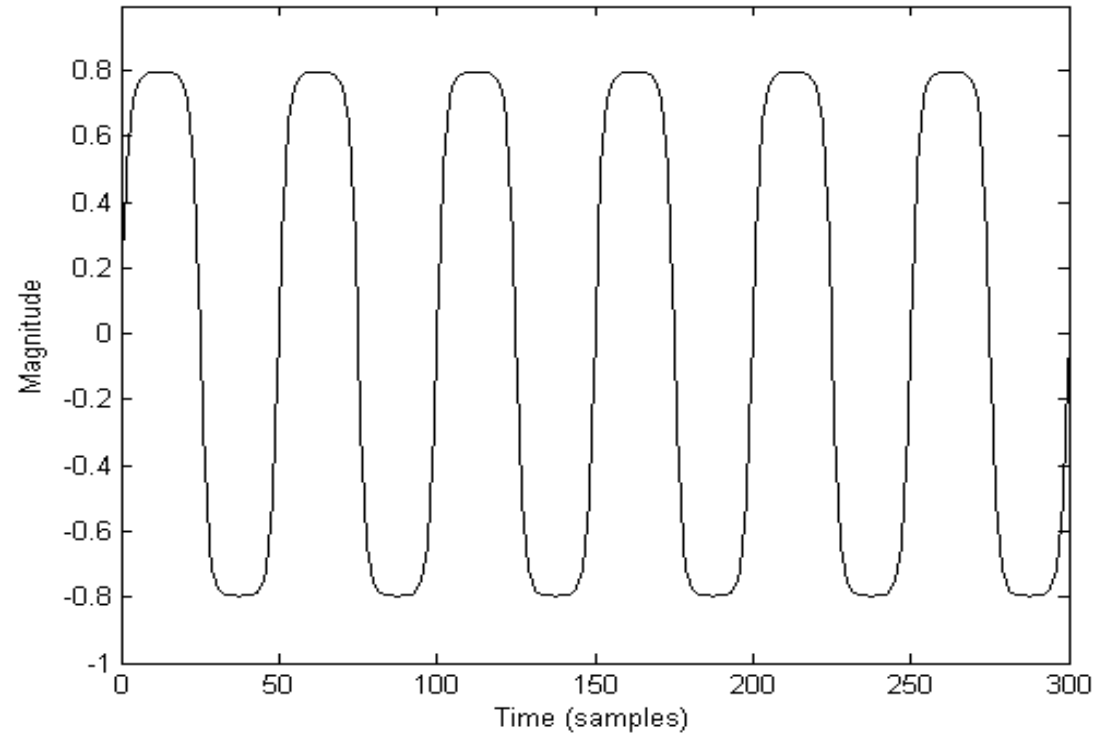

(a)

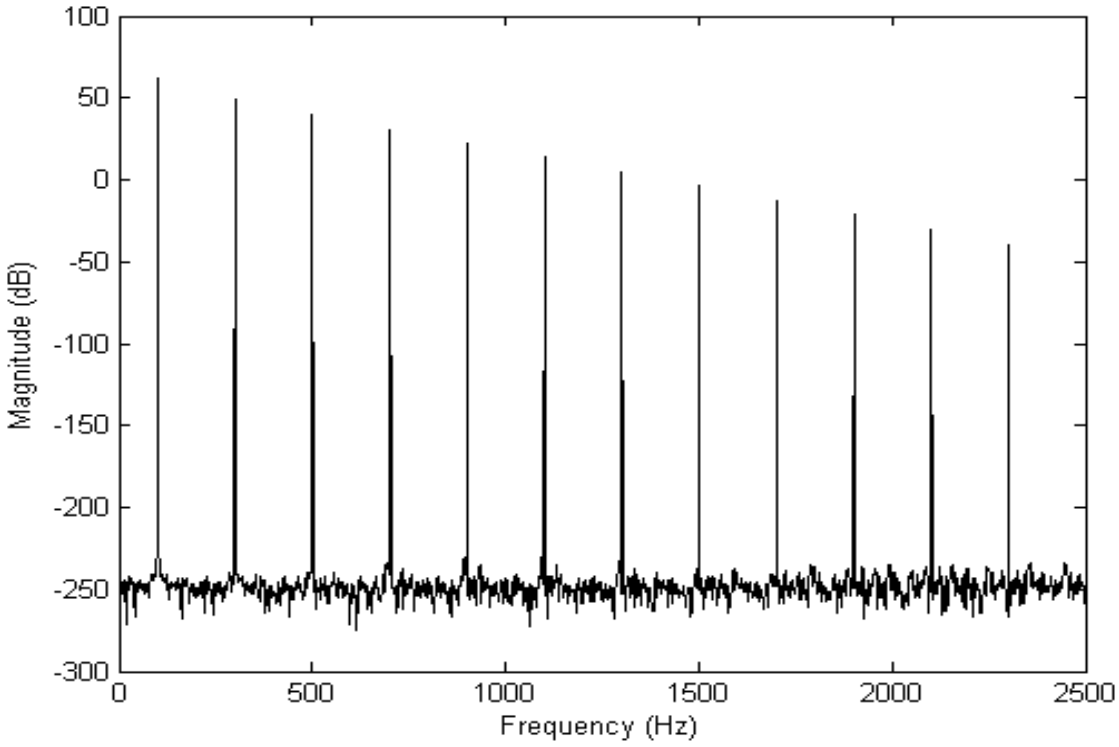

(b)

Fig. 3 The transform of a sine wave 100 Hz on the time and frequency domains by the methods of hyperbolic tangent. (a) time domain (b) frequency domain.

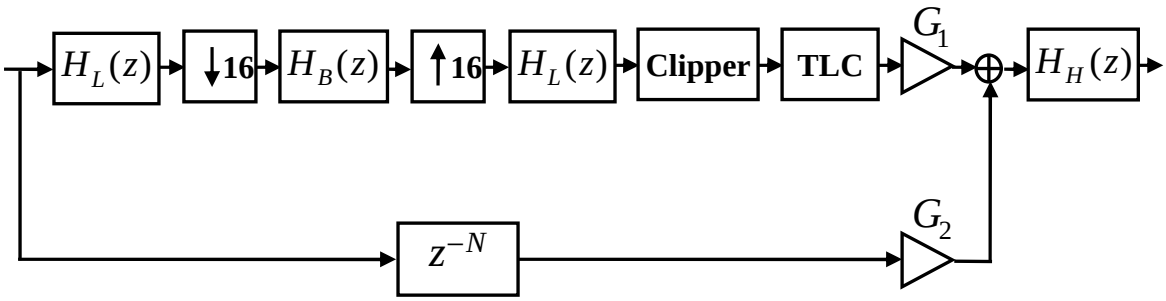

Fig. 4 The complete Structure of virtual bass realization.

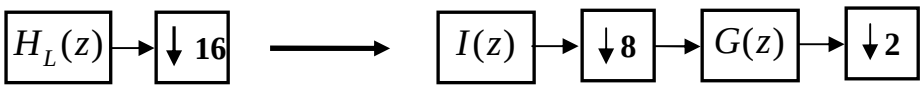

(a)

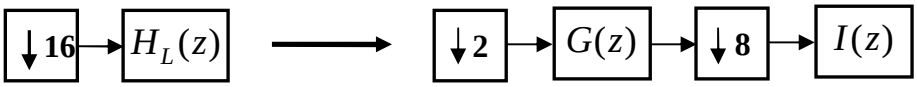

(b)

Fig. 5 The two-stage decimation (a) and interpolation filters (b) developed from the IFIR technology.

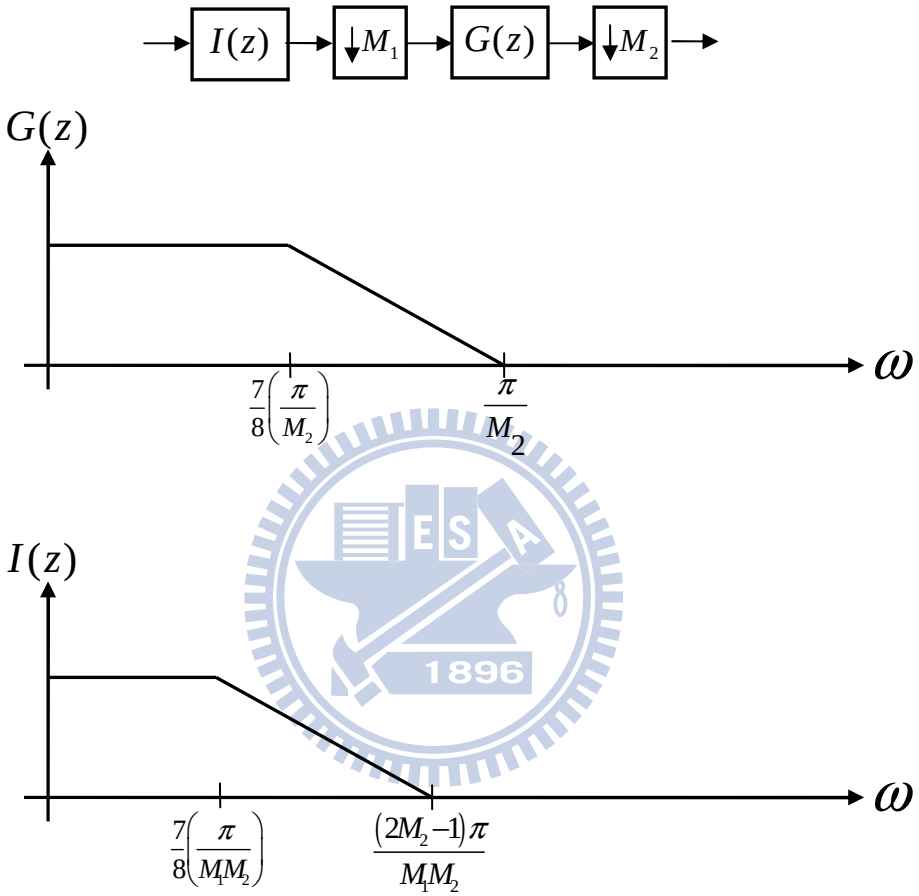

Fig. 6 The implementation of up/down-sampling using the multistage structure.

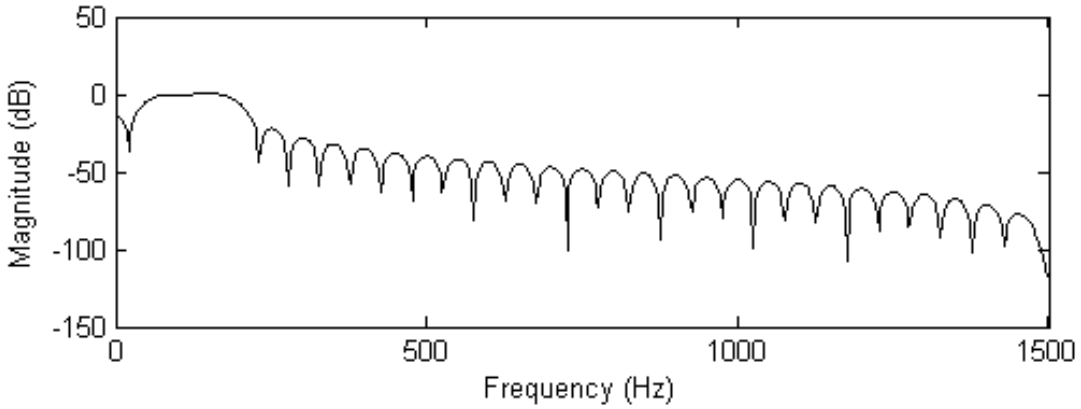

(a)

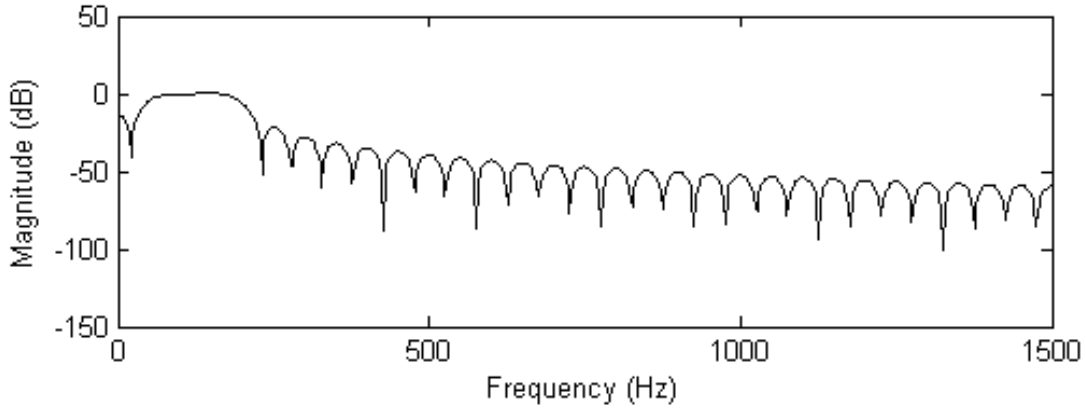

(b)

Fig. 7 Band pass filter (a) 60 filter order (b) 960 filter order.

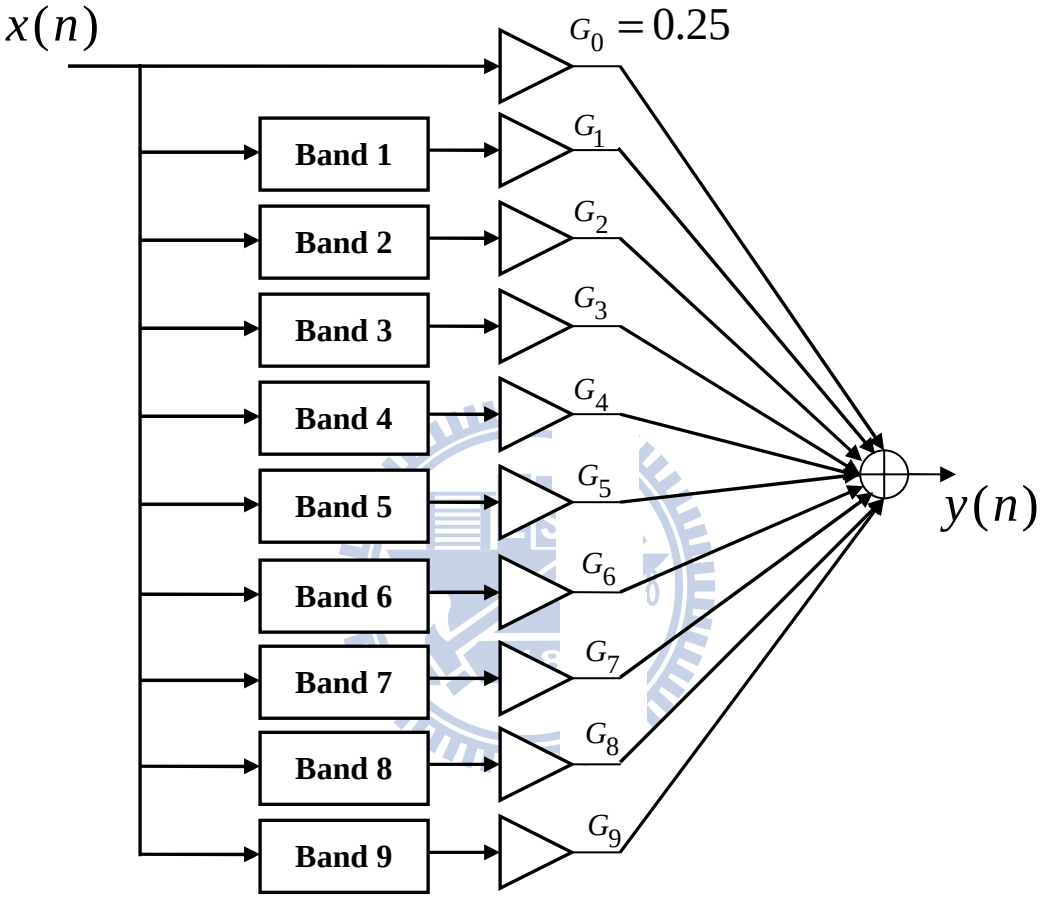

Fig. 8 The implementation structure of a 9-band of Graphic equalizer.

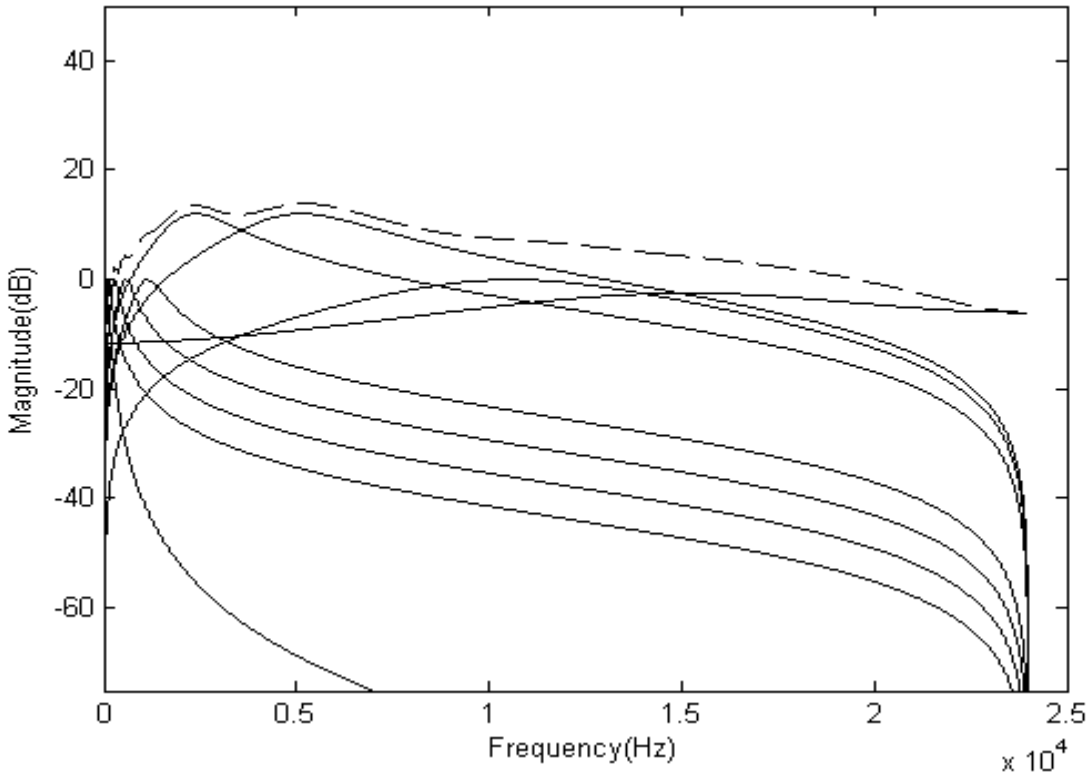

Fig. 9 The frequency response of graphic equalizer after boosting 12dB between 1.6Hz to 7.2Hz.

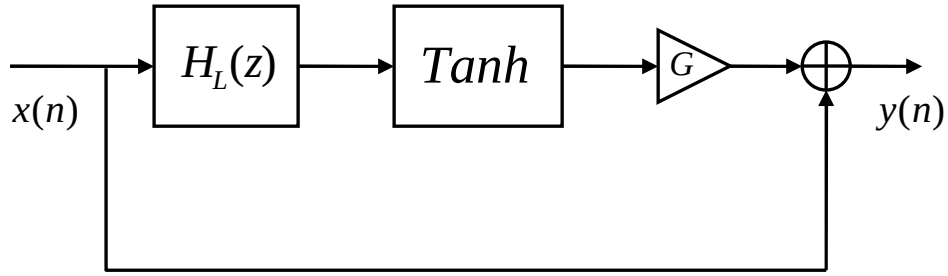

(a)

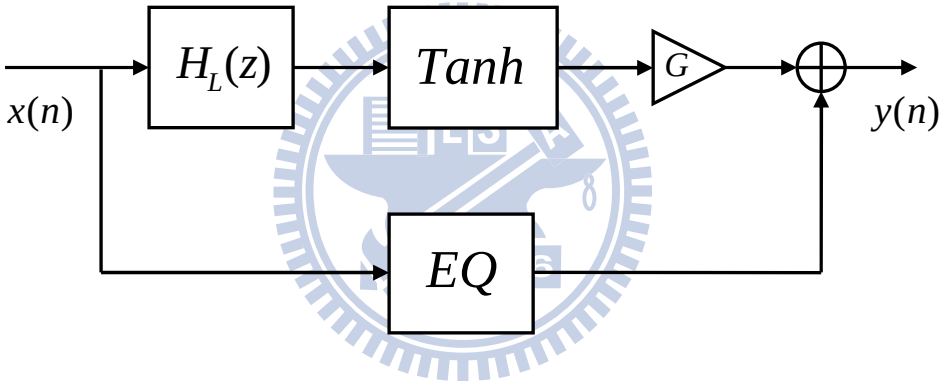

(b)

Fig. 10 The implementation structure of voice clarity (a) The structure using hyperbolic tangent (b) The structure using hyperbolic tangent and graphic equalizer

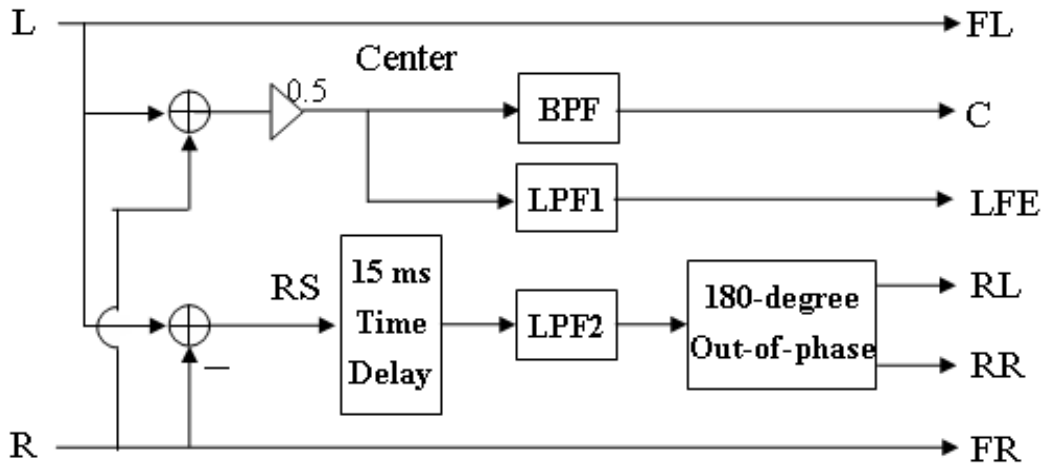

Fig. 11. General architecture of upmix processing for producing surround and center channels.

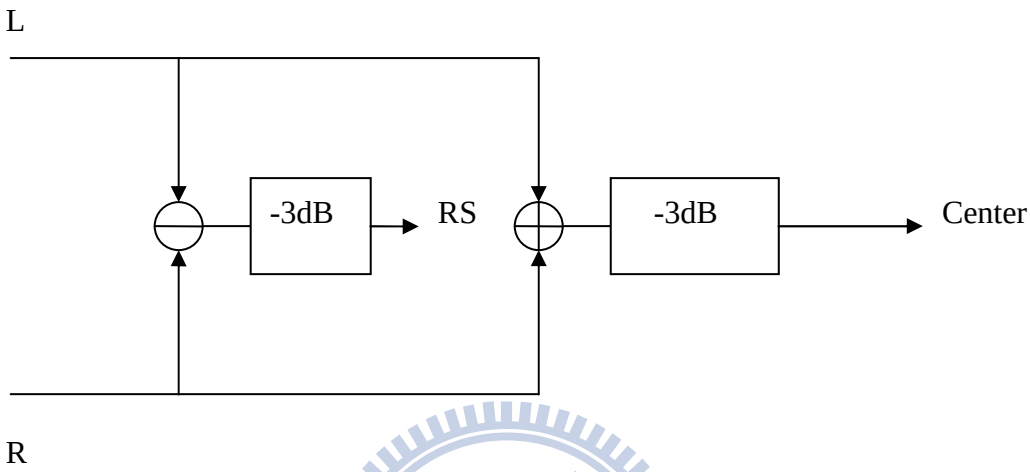

Fig. 12. The block diagram of the passive surround decoder method.

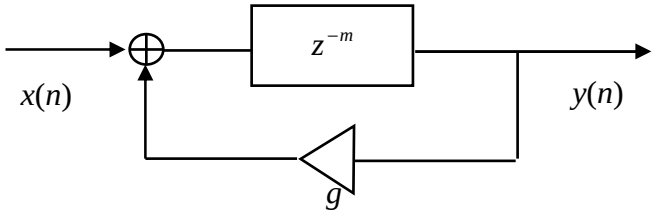
z^{-m}
$x(n)$
$y(n)$
g

(a)

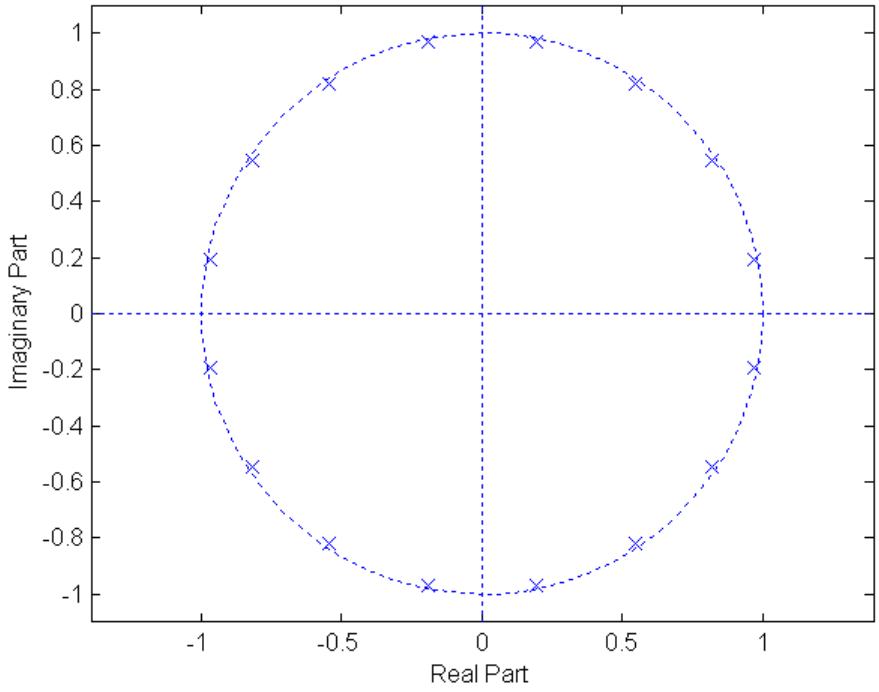
Imaginary Part
Real Part
1
0.8
0.6
0.4
0.2
0
-0.2
-0.4
-0.6
-0.8
-1
-1
-0.5
0
0.5
1

(b)

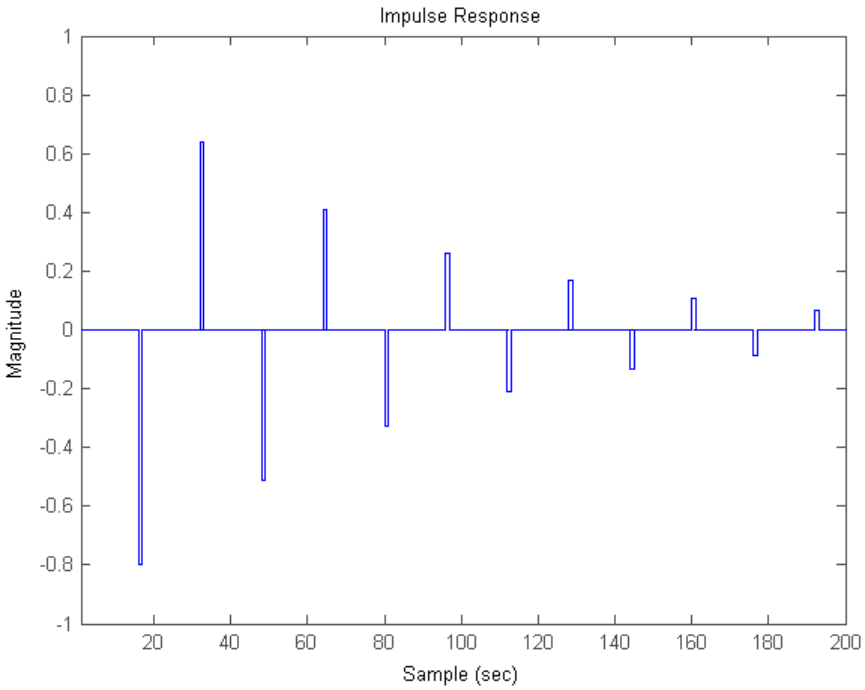

(c)

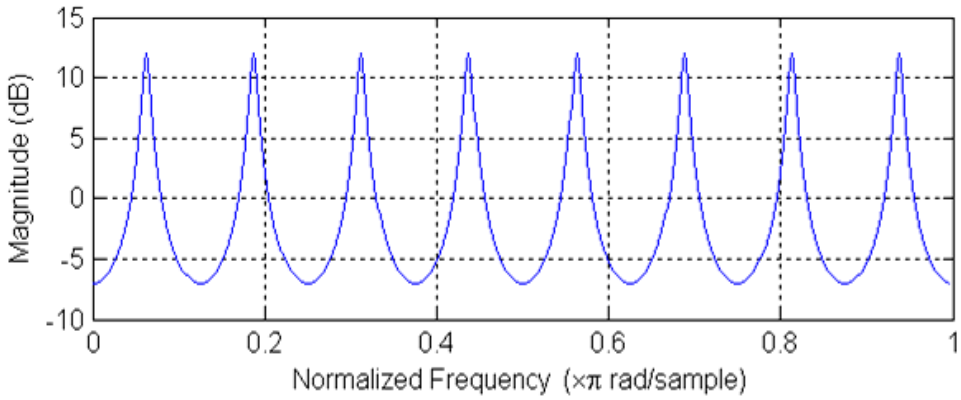

(d)

Fig. 13. Comb filter. (a) Block diagram. (b) Zero-pole plot. (c) Impulse response. (d) Frequency response.

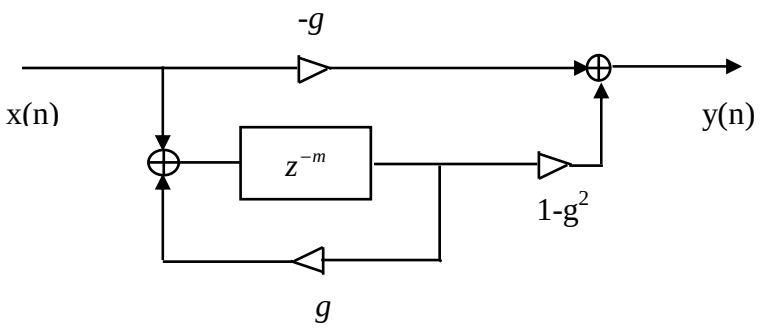

Figure 4. (a)

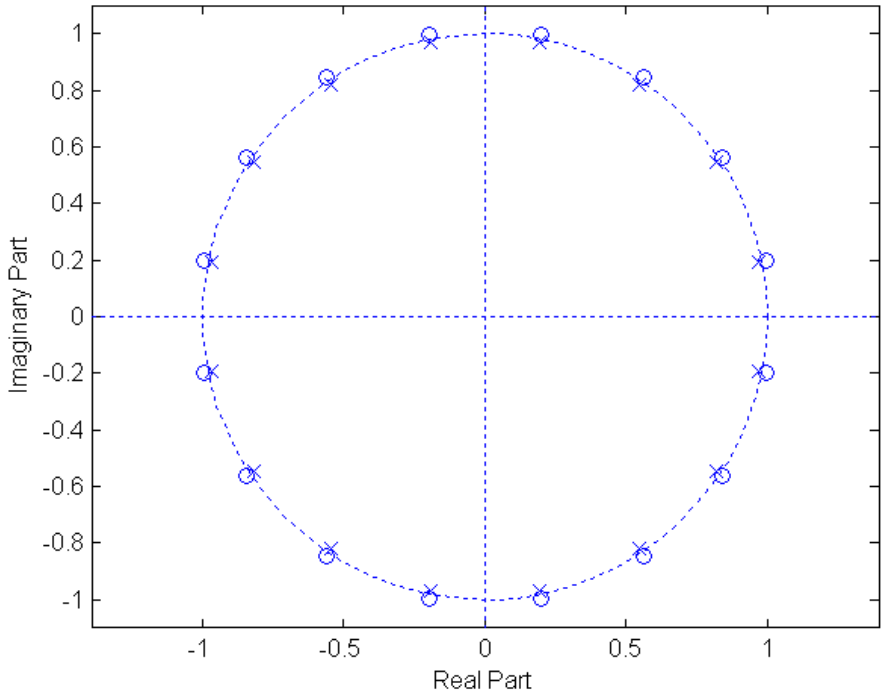

Figure 4. (b)

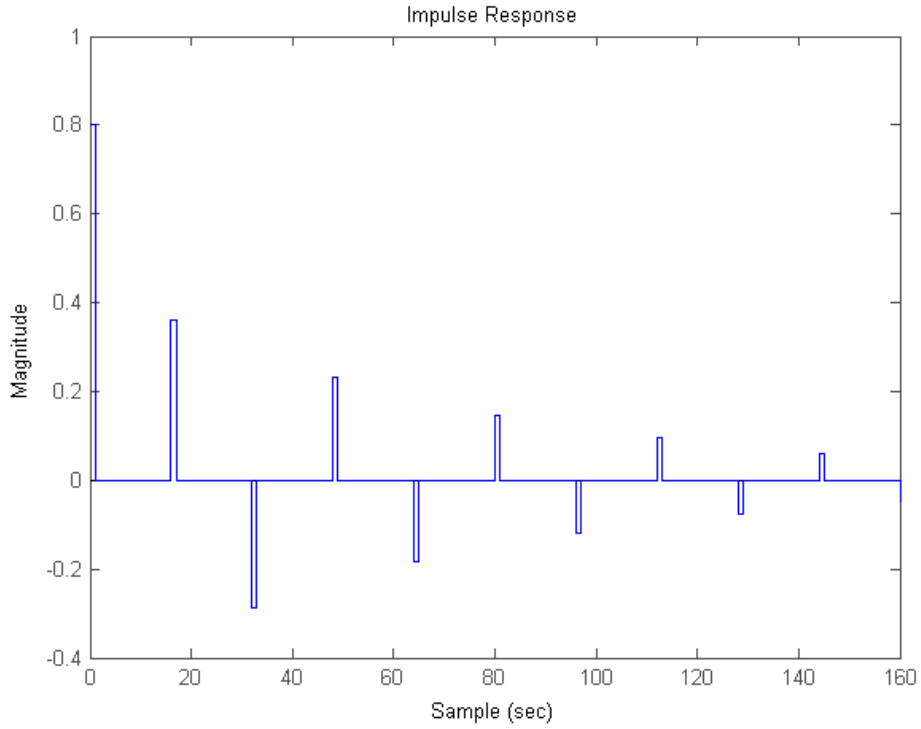

Figure 4. (c)

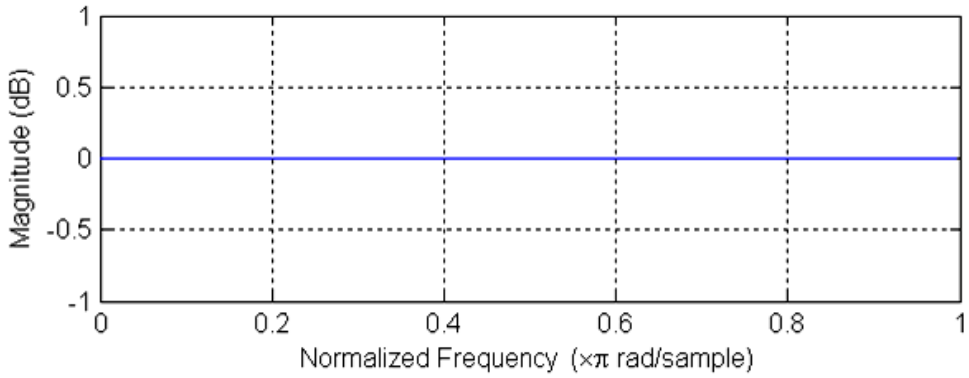

Figure 4. (d)

Fig. 14. All-pass filter. (a) Block diagram. (b) Zero-pole plot. (c) Impulse response. (d) Frequency response.

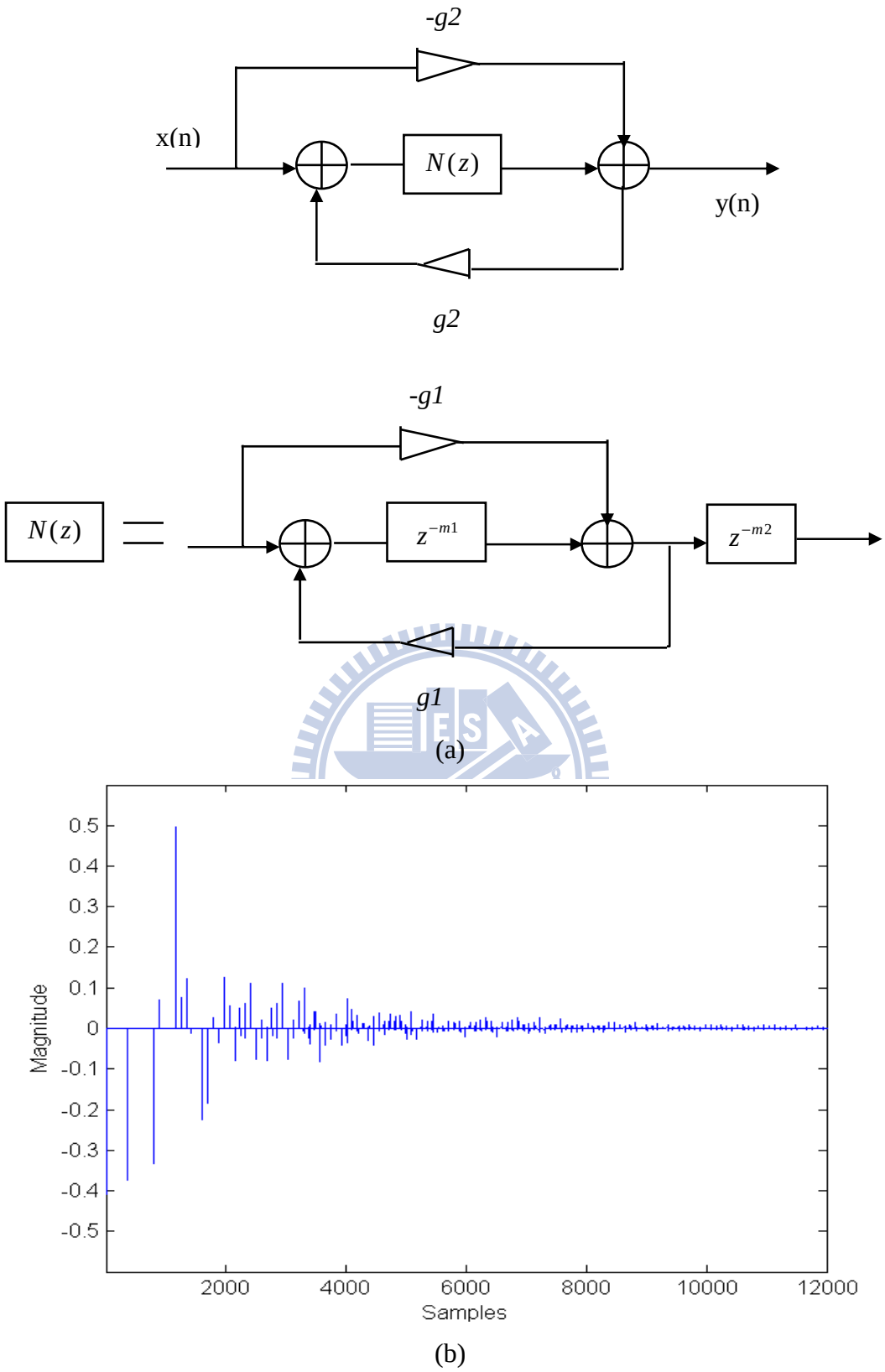

Fig. 15. Nested all-pass filter. (a) Block diagram (b) Impulse response of the three-layer nested all-pass filter with $g_1 = 0.5,\ g_2 = 0.45,\ g_3 = 0.41$ and delay lengths $m_1 = 441,\ m_2 = 533,\ m_3 = 617$.

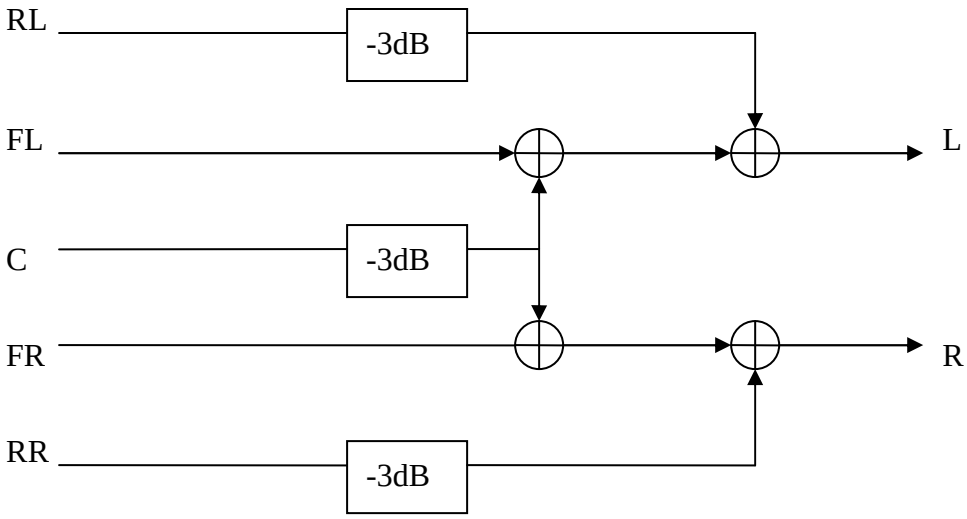

Fig. 16. The architecture of the standard downmix method.

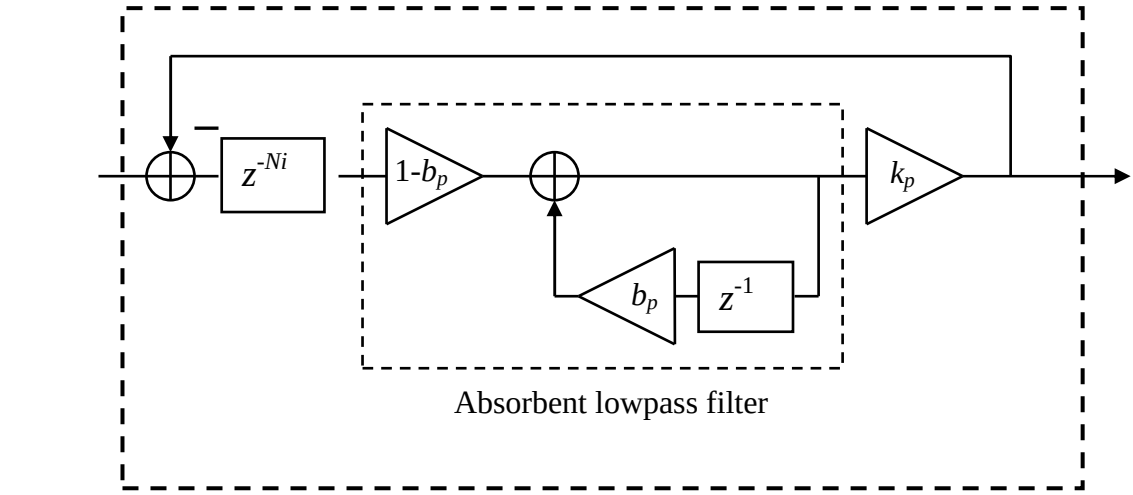

(a)

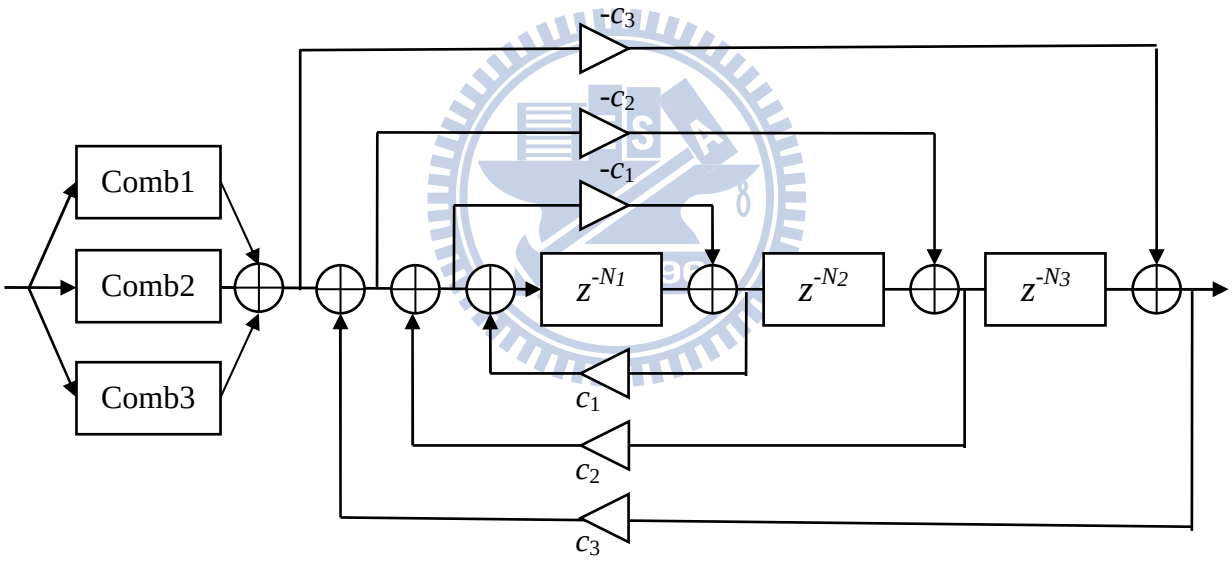

(b)

Fig. 17. (a) The artificial reverberator is constructed from 3 parallel comb filters. (b) 3-layered nested-allpass filter.

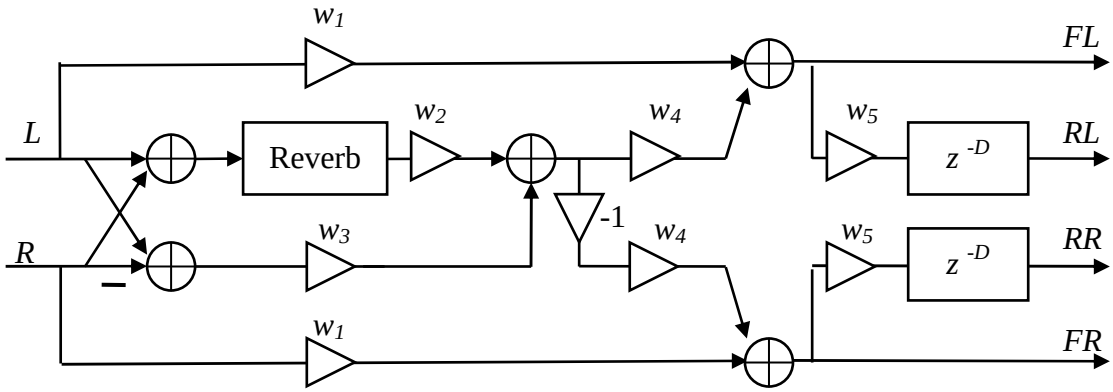

Fig. 18. The block diagram of the reverberation-based upmix processing.

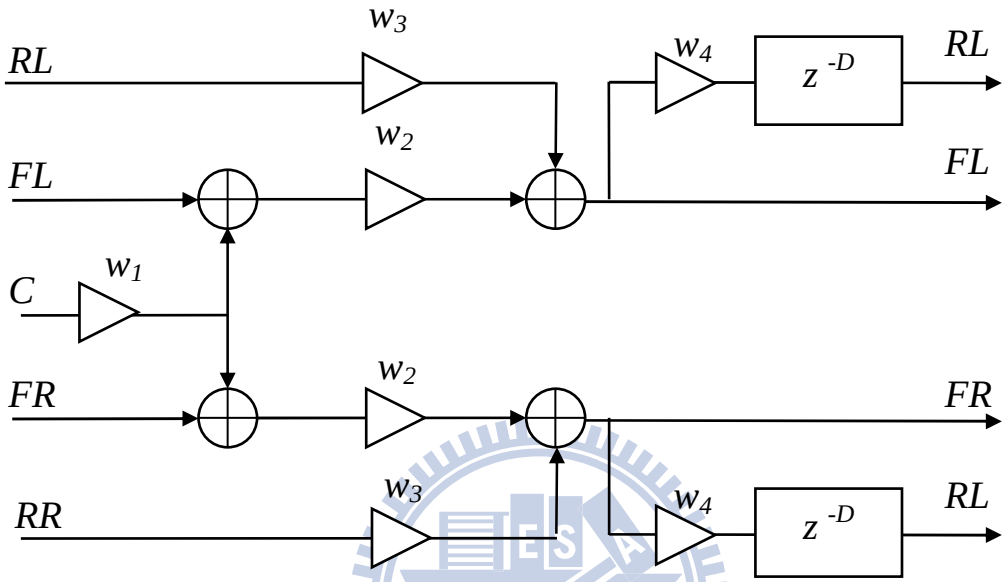

Fig. 19. The block diagram of the standard downmix adding weighting and delay.

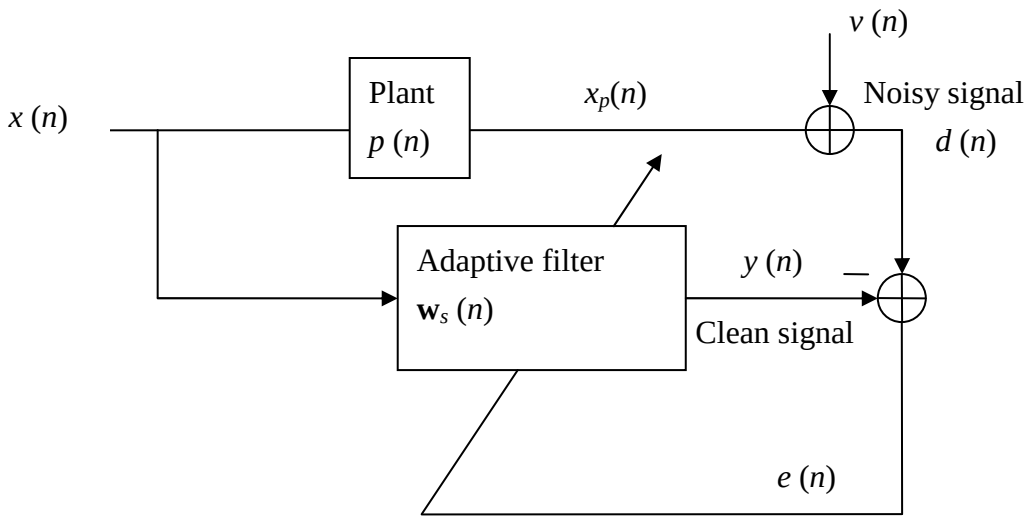

Fig. 20 The structure of the noise level estimation system.

.

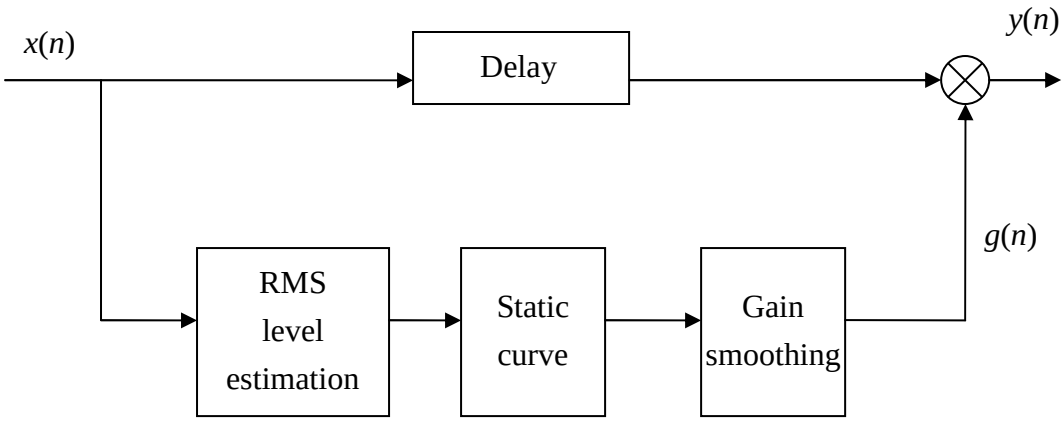

Fig. 21 The block diagram of the dynamic range control system.

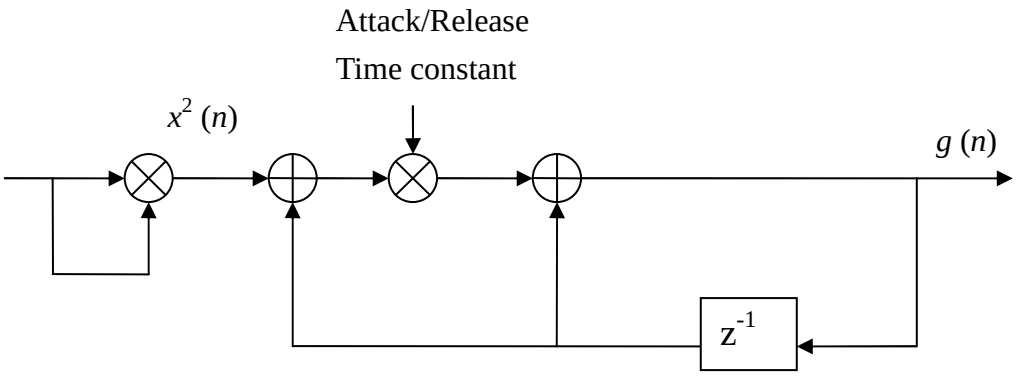

Fig. 22 The RMS measurement.

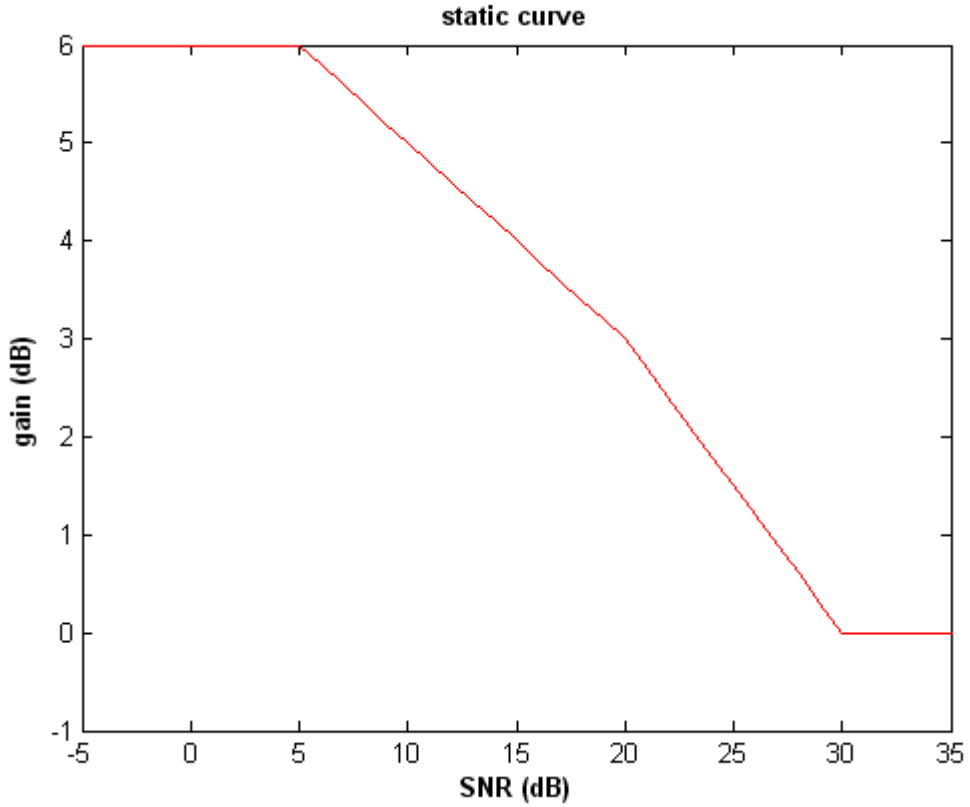

Fig. 23 The static curve which is designed for using the SNR to calculate the output gain.

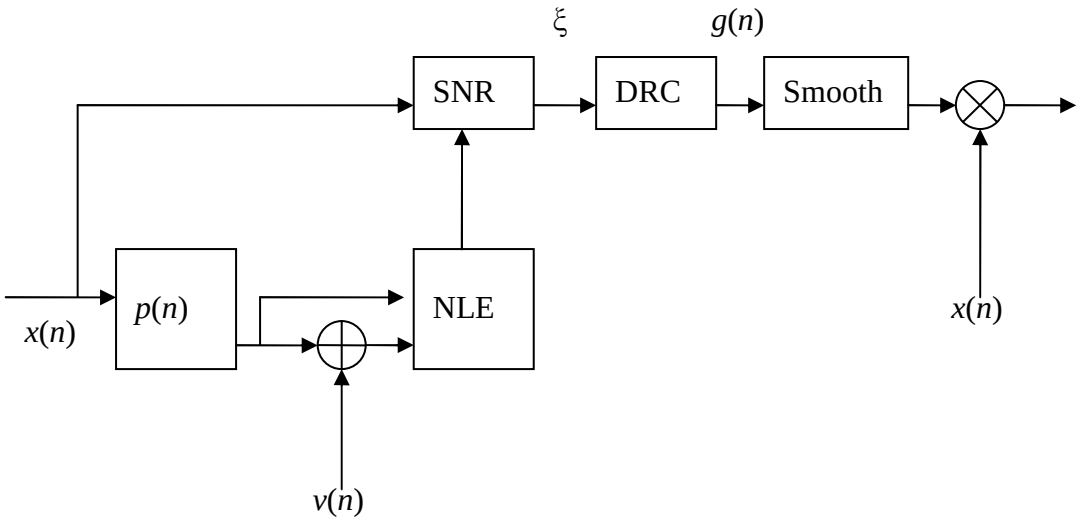

Fig. 24 The block diagram of the adaptive gain control system.

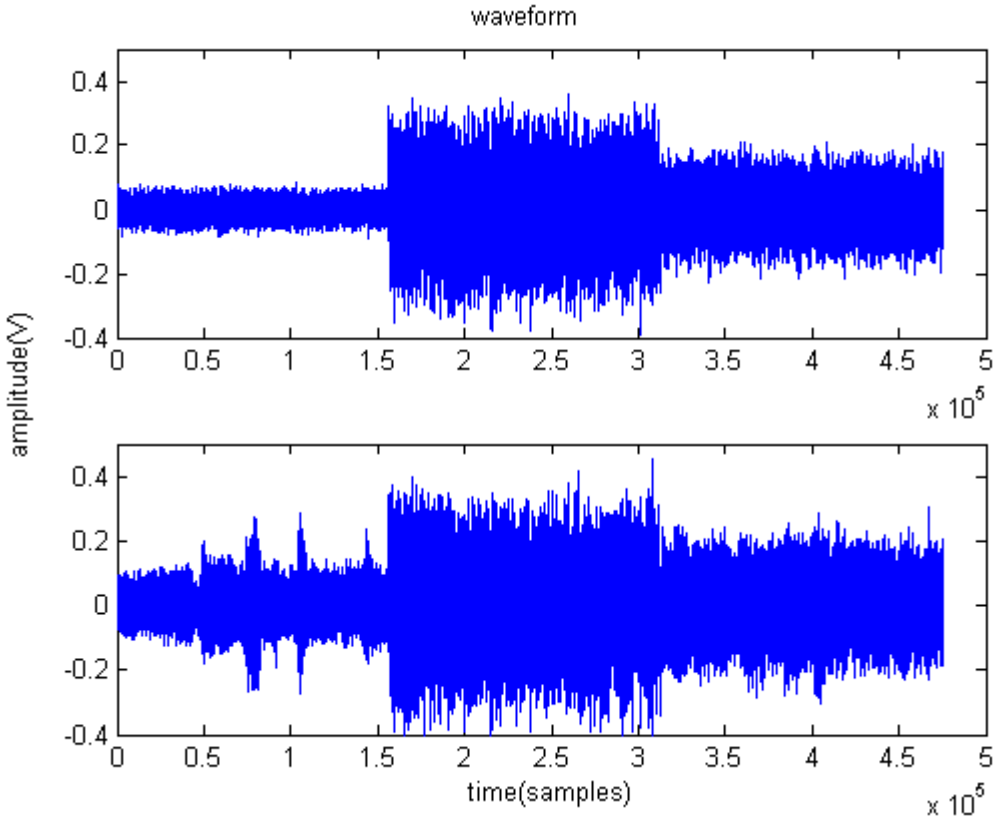

Fig. 25 The level varying whitenoise. The upper row is the original noise. The lower row is the estimated noise.

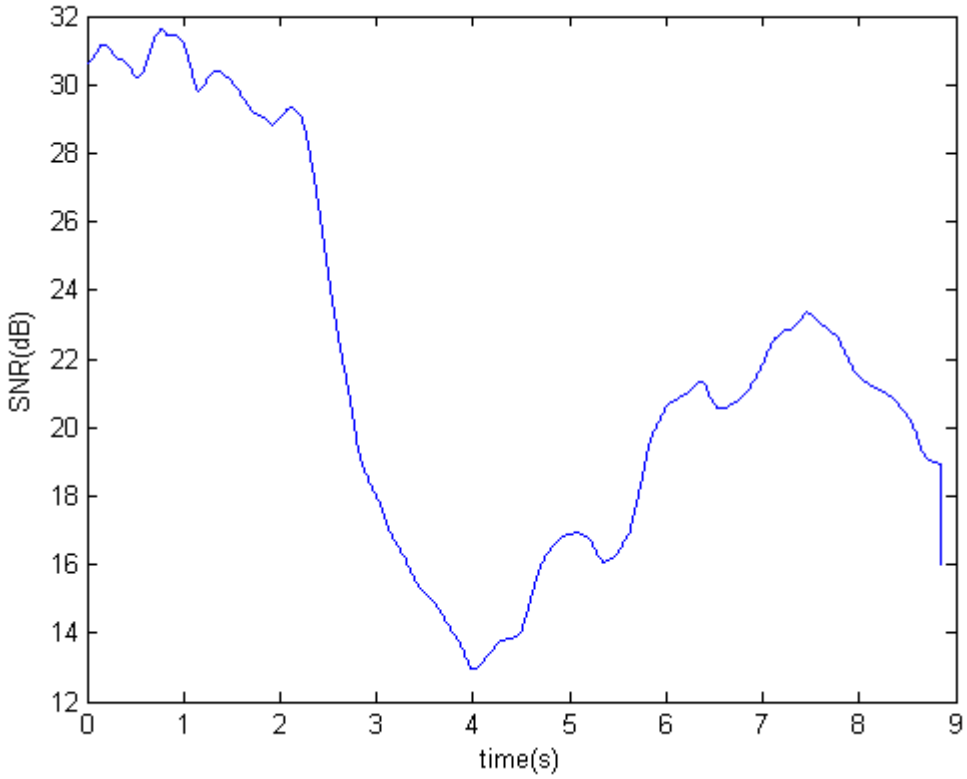

Fig. 26 The SNR which is calculated by a signal and a level varying whitenoise.

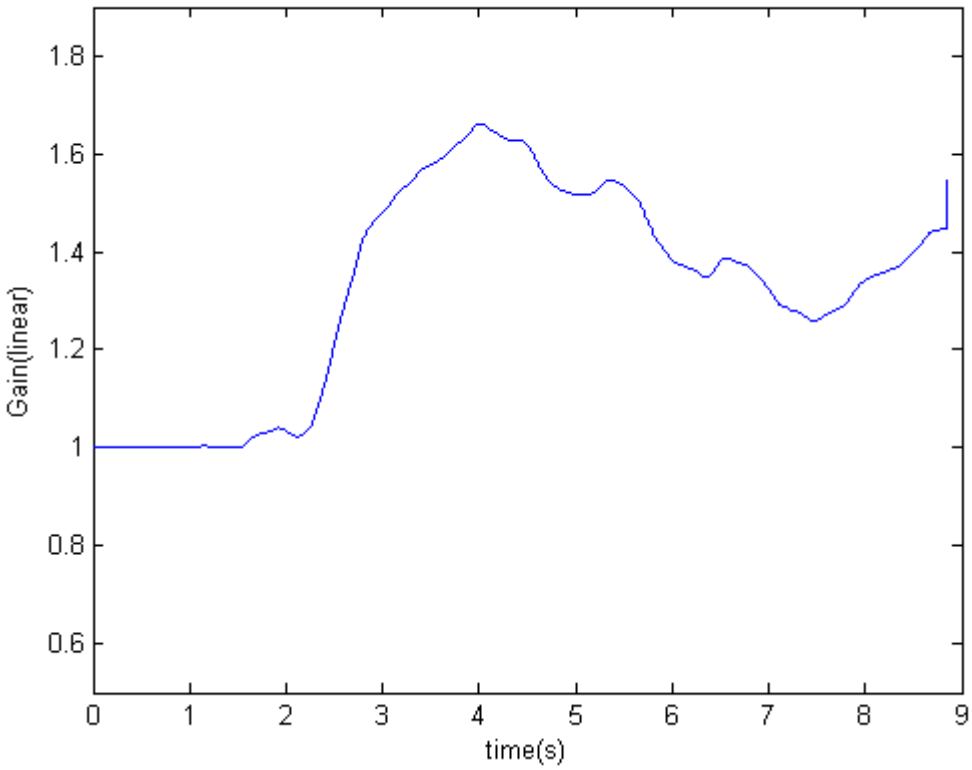

Fig. 27 The output gain.

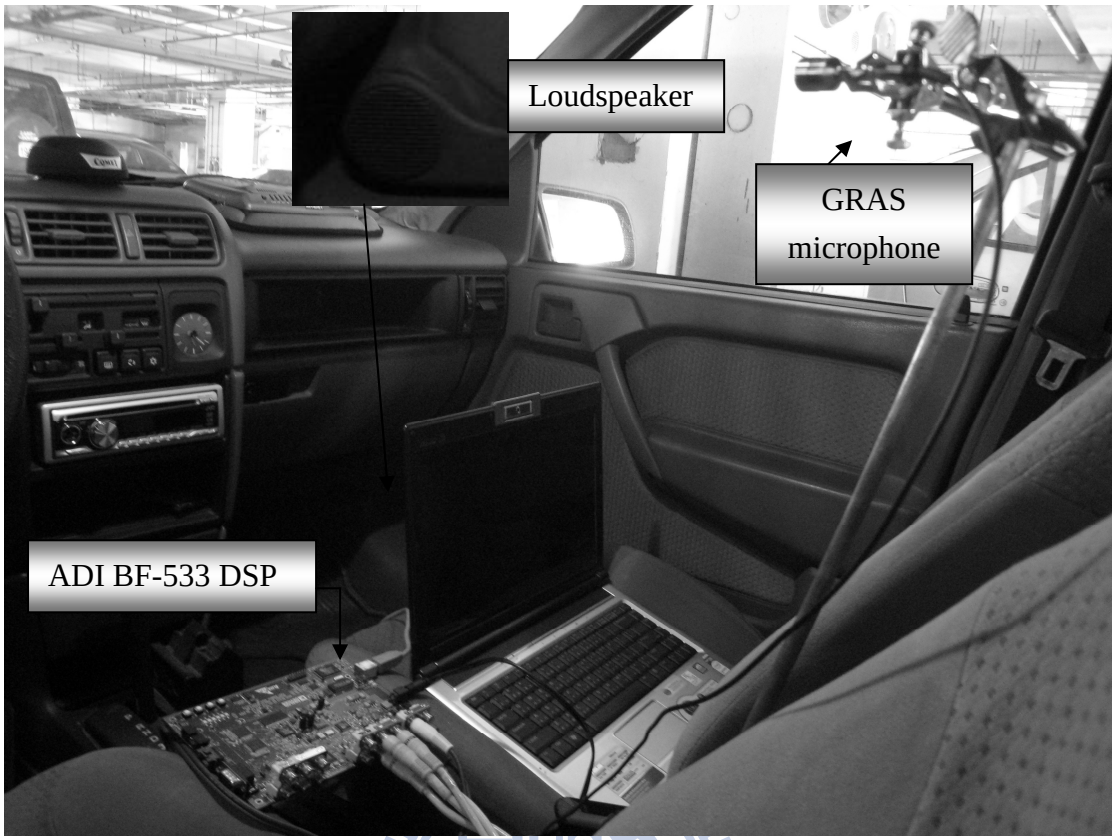

Fig. 28 The experimental arrangement.

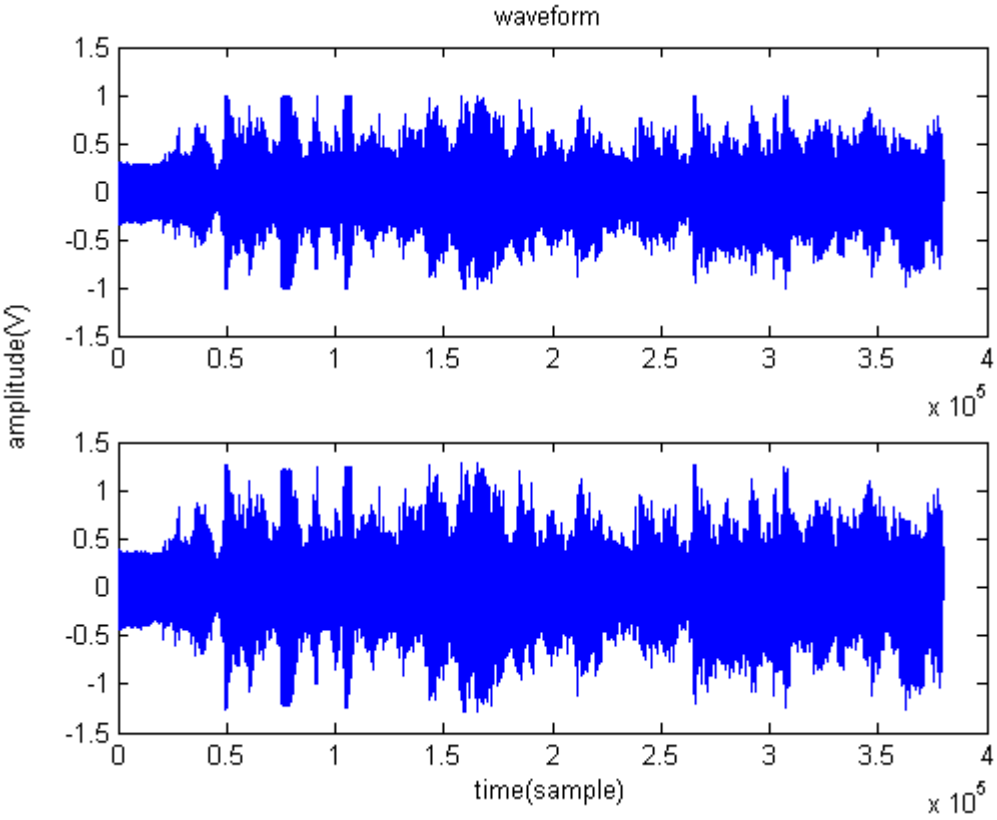

Fig. 29 The waveform of case 1. The upper row is the waveform when system off. The lower row is the waveform when system on.

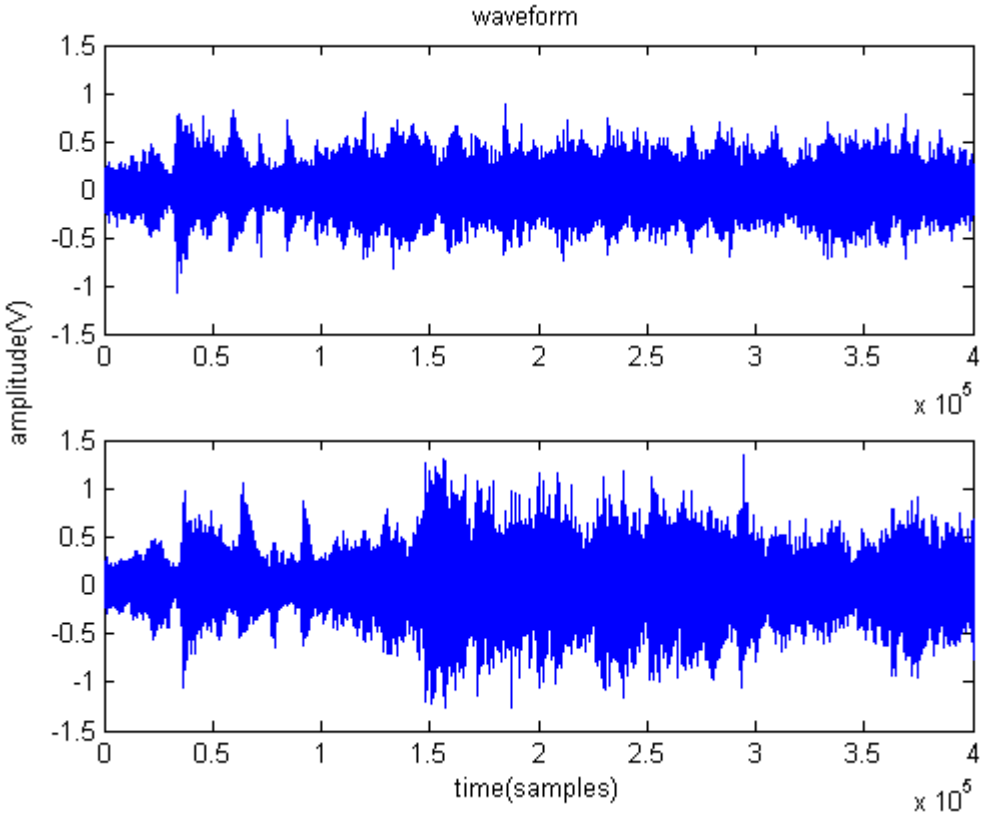

Fig. 30 The waveform of case 2. The upper row is the waveform when system off. The lower row is the waveform when system on.